NBER WORKING PAPER SERIES

IMPLICATIONS OF STOCHASTIC TRANSMISSION RATES FOR MANAGING PANDEMIC RISKS

Harrison Hong
Neng Wang
Jinqiang Yang

Working Paper 27218
http://www.nber.org/papers/w27218

NATIONAL BUREAU OF ECONOMIC RESEARCH
1050 Massachusetts Avenue
Cambridge, MA 02138
May 2020

We thank Patrick Bolton, Ing-Haw Cheng, Marcin Kacperczyk, Je rey Kubik, Harry Mamaysky, Sen Pei, Stijn Van Nieuwerburgh, Laura Veldkamp, and seminar participants at Columbia COVID-19 Virtual Symposium, Columbia Finance, and Imperial College London for helpful comments.The views expressed herein are those of the authors and do not necessarily reflect the views of the National Bureau of Economic Research.

Implications of Stochastic Transmission Rates for Managing Pandemic Risks
Harrison Hong, Neng Wang, and Jinqiang Yang
NBER Working Paper No. 27218
May 2020, Revised June 2020
JEL No. G12,G32,Q5

ABSTRACT

The reproduction number R_0 plays an outsized role in COVID-19 risk management. But it is an insufficient statistic, particularly for financial risks, because transmissions are stochastic due to environmental factors. We introduce aggregate transmission shocks into a widely-used epidemic model and link firm valuation to epidemic data by using an asset-pricing framework that accounts for potential vaccines. Pooling early data, we estimate a large R_0 and transmission volatility. R_0 mismeasures social-distancing benefits because it gives a poor approximation of conditional infection forecasts. R_0 mismeasures financial risks since transmission volatility and vaccine news also determine firm-value damage.

Harrison Hong
Department of Economics
Columbia University
1022 International Affairs Building
Mail Code 3308
420 West 118th Street
New York, NY 10027
and NBER
hh2679@columbia.edu

Jinqiang Yang
Shanghai University of Finance
and Economics
Guoding Rd. 777
Shanghai, 200433
China
yang.jinqiang@mail.sufe.edu.cn

Neng Wang
Columbia Business School
3022 Broadway, Uris Hall 812
New York, NY 10027
and NBER
nw2128@columbia.edu

1 Introduction

The basic reproduction number $\mathcal{R}_0$, defined as the expected number of secondary infections generated by a single (representative) infected individual in a fully susceptible population, plays an outsized role in managing COVID-19 risks. On the public health front, leading large-scale computational epidemiological models emphasize that $\mathcal{R}_0$ is greater than one and recommend lockdown measures to keep the reproduction number below one (see, e.g., Ferguson et al. (2020), Kucharski et al. (2020), and Li et al. (2020)).

On the economic front, an emerging macroeconomic literature focuses on economic trade-offs—the costs to flatten the curve—and conducts policy analysis (e.g., Alvarez, Argente and Lippi (2020), Atkeson (2020), Eichenbaum, Rebelo and Trabant (2020), and Gourinchas (2020)). These papers take $\mathcal{R}_0$ estimates from leading epidemiological studies in generating infection forecasts from deterministic epidemic models that economic agents use as a counterfactual infection scenario absent interventions such as social distancing. Interventions are assumed to vary $\mathcal{R}_0$ and hence flatten the forecasts of infections from a deterministic model.

Largely ignored is that estimates of $\mathcal{R}_0$ come with wide standard error bands, as we show below. Such wide bands are not simply due to innocuous measurement error. Rather, a large epidemiology literature (see Andersson and Britton (2012)) points to aggregate transmission rate shocks reflecting super-spreading events such as mass gatherings, weather events that inhibit or promote transmission, or changes in social interactions that govern contact rates.

We show that $\mathcal{R}_0$ is an insufficient statistic for managing COVID-19 risks, be it health or economic, because aggregate transmission volatility is significant. This is particularly the case when one considers financial risks of the sort mentioned by the Federal Reserve Board Financial Stability Report (2020): "Asset prices remain vulnerable to significant price declines should the pandemic take an unexpected course..." That is, economic and financial modeling of pandemics needs to feature an epidemic model with stochastic transmission shocks that agents can use to generate counterfactual forecasts for infections.

Towards this end, we consider an extension of a widely-used deterministic epidemic model of COVID-19 (Kermack and McKendrick (1927)) featuring aggregate transmission-

rate shocks that are intended to capture that viral contagiousness is unpredictable due to environmental factors.[1] Epidemic models of COVID-19 typically entertain multiple compartments in terms of tracking susceptible, infected, and resistant (including the recovered and dead). In order to transparently highlight the importance of transmission volatility, we focus on modeling just the infected population I_t, via a susceptible-infected-susceptible (SIS) as opposed to a susceptible-infected-recovered (SIR) setting.[2] There is also no consensus at this point that COVID-19 infection confers long-lasting immunity. For a number of economic and financial applications, the focus is typically on horizons of many years and the infected population is often the main state variable of interest since damages are likely to be proportional to infections.

We model the aggregate transmission shocks via a stochastic transmission rate, $\widetilde{\beta}$. This key input is modeled as a random variable with constant mean (predictable transmission captured by parameter β) and transmission shocks (mean zero but with volatility captured by parameter σ).[3] The exit rate from the infected state back into the susceptible state is additionally assumed to be a constant γ. The resulting dynamics of the fraction of infected then follows a three-parameter non-linear diffusion process.

We calculate analytical conditional distributions from the Kolmogorov forward equation associated with our epidemic process to characterize the transition risk of epidemics. In the limit of no volatility, our model becomes the deterministic SIS model solution. While it is understood by mathematical epidemiologists that introducing noise into the transmission process will lead to a dampening of stationary distribution of infections,[4] we show that the inherent value of this parsimonious model lies in the characterization of the conditional distributions up to a differential equation including the stationary distribution.

[1] By environmental factors, epidemiologists broadly refer to weather, behavioral, cultural, and geographical factors.

[2] This SIS setting is useful for modeling viruses where recovery does not grant long-lasting immunity, which includes potentially many types of viruses.

[3] This parameter perturbation approach has been used in the mathematical epidemiology literature (see, e.g., Gray et.al. (2011)) and in statistical models of epidemics (see, e.g., Dureau et.al. (2013)).

[4] See Andersson and Britton (2012) and Brauer, Driessche, and Wu (2008). Even if the reproduction number $\mathcal{R}_0 > 1$, the epidemic process might nonetheless die out due to the uncertainty of transmissions as opposed to in the deterministic setting.

We can compare the infection forecasts from this stochastic epidemic model (which depends on β, γ and σ) to those generated by a deterministic model which depends just on $\mathcal{R}_0$, i.e. the ratio of β to γ. Moreover, we tractably introduce a stochastic vaccine arrival to our epidemic model as a jump with a Poisson arrival rate. When the vaccine arrives, we assume the epidemic is over and infections go to zero. Hence, we can also calculate conditional forecasts assuming different vaccine arrival rates λ.

We then model the financial impact of infection forecasts through the lens of a dynamic asset-pricing model. We allow COVID-19 to impact both the drift and volatility of an asset's earnings process as well as the market price of pandemic risk. The stochastic discount factor (SDF) during a pandemic should depend not just on business-as-usual shocks but also aggregate transmission shocks and stochastic vaccine arrival. We obtain a generalized dividend discount model (as a special case of our asset-pricing model) that allows infections to adversely affect earnings. Our pricing formula transparently links valuation to epidemic data (infections, reproduction numbers, transmission volatility, and vaccine arrival rate). This formula allows us to assess the valuation damage of COVID-19 under infection forecasts from a deterministic model versus our stochastic epidemic model.

We can straightforwardly estimate our epidemic model by pooling COVID-19 case data from 16 countries (regions) that are at high risk during the period of January - February of 2020. These countries had among the most air travel connections to the city of Wuhan in China and have been the basis of the modeling of the early dynamics of COVID-19 absent government lockdowns. Given the noisiness and brief time series of the data and our goal of demonstrating the influence of shocks, we fit one model for all 16 countries.

Our estimate of β is 6.62 per month, which translates to an infected individual infecting one susceptible on average every five days ($\approx 30/6.62$.) Our estimate of monthly σ is 1.69, which translates to a standard deviation of plus or minus 1.69 individuals per month. The exit rate γ is equal to the inverse of the expected duration that an infected is sick and infective; it is typically not estimated based on aggregate data early in epidemics since there is a delay in when individuals leave the infected state. There is no consensus on this number.[5]

[5]It ranges from around 7 days to 14 days at the individual level but with a fat-tail in terms of an infectious

For our estimation of a population average, we simply use 14 days as the duration to infer the exit rate γ at $1/(14\,\text{days})$, which is 2.17 per month. But we also consider 10 days as a robustness check.[6]

These estimates then imply that our (basic) reproduction number $\mathcal{R}_0$ using case data from January-February is 3.05 and the 90% confidence interval (CI) is (1.12, 6.52) based on the empirical distribution. The wide standard errors of course reflect our significant estimate of σ. Despite constraining one model for all countries (regions), our estimates are in line with leading studies of COVID-19.[7] Using these estimates, we then calculate the analytical conditional distributions for the fraction of infected for each of the 16 countries (regions) in March-April taking as an initial condition the fraction infected in each country at the beginning of March.[8] Our epidemic model generates sensible out-of-sample forecasts in line with leading epidemiological studies.[9]

But the value of our model lies in its implications for managing COVID-19 risks. We assess the economic and financial damage along side damage to health from COVID-19 in a couple of ways. We input parameter estimates form January-February 2020 and contrast infection and valuation forecasts from the deterministic and stochastic models. We can also vary the key parameters of $\mathcal{R}_0$ and σ^2 — these infection and valuation forecasts can be used by agents to assess intervention scenarios in the spirit of Atkeson (2020) and Gourinchas (2020).

To start, $\mathcal{R}_0$ and forecasts generated by a deterministic epidemic model mismeasures the benefits of economy-wide lockdowns, especially modeled in the recent macroeconomic literature on flattening the curve highlighted above. There are two reasons for why this

period across individuals.

[6] In leading models, this parameter is typically assumed to follow an Erlang distribution (Kucharski et al. (2020)).

[7] Kucharsi et al. (2020) estimate a reproduction number of 2.35 [95% CI 1.15-4.77], while Imai et al. (2020) estimate that it is 3.1 [95% CI 1.7-4.3].

[8] Recently, Fernandez-Villerde and Jones (2020) estimate epidemic processes focusing on death rates while Toda (2020) estimates a SIR epidemic model for COVID-19 allowing for heterogeneous transmission rates across regions. Our SIS model in contrast focuses on how volatility affects transition dynamics and how health and financial outcomes depend on volatility of transmission rates.

[9] Following these studies, our baseline infection forecasts assume that the vaccine arrival rate is set to zero since a viable vaccine is not expected for several years.

is the case. The first reason is that $\mathcal{R}_0$ does not capture initial transmission shocks being permanent. When the initial fraction of infected is low, the I_t process is approximately a Geometric Brownian motion with outsized drift β and volatility σ parameters. This means that shocks early on have permanent and very large effects. The permanence of initial shocks can explain why a large amount of the variance in 1918 Flu spatial outcomes cannot be explained (see Almond (2006) for a review of the evidence). It can also explain why early action on social distancing might be useful in shutting down stochastic transmission shocks (Adda (2016), Fang, Wang and Yang (2020), Hsiang et al. (2020)).

Second, deterministic model infection forecasts based on $\mathcal{R}_0$ are poor approximations of our model's conditional forecasts. For instance, when $\mathcal{R}_0$ is 1.75, the conditional mean forecast is 0.05 and the conditional standard deviation is 0.135 at 24 months out. In contrast, a deterministic model would forecast 42.9% of the population would be infected at the same horizon. Another way of framing this overshooting is that while discussions regarding government interventions have focused on bringing the reproduction number below one, our analytical conditional distribution calculations suggest that even at a fairly high reproduction number $\mathcal{R}_0$ such as 1.75 COVID-19 will likely be a slow burn as opposed to an outbreak.

A key piece of intuition for this result comes from Gray et al. (2011) who characterize the stationary distribution of our non-linear diffusion process absent a vaccine. Whereas $\mathcal{R}_0 > 1$ determines epidemic outbreak in a deterministic model, the analogous outbreak point $\overline{\mathcal{R}}_0$ is equal $(\beta - \sigma^2/2)/\gamma$ in our stochastic model. Therefore, even at a reproduction number $\mathcal{R}_0$ above 1, an epidemic cannot be sustained when σ^2 is large.

Since the infection forecasts are significantly different across the deterministic and stochastic models, forecasts of damage to valuation will of course also differ markedly. That is, $\mathcal{R}_0$ not only mismeasures the benefits of economy-wide lockdowns but also misestimates COVID-19 damage to financial markets. Indeed, our fundamental asset pricing formula highlights not just the role of the reproduction number of COVID-19 but how its transmission volatility influences valuations via at least three channels: 1) earnings growth effect; 2) the convexity effect of pandemic risk; and 3) the risk premium channel. The risk premium channel arises since COVID-19 has an impact on aggregate consumption (wealth) and hence the price of

COVID-19 risk determines the discount rate applied to cashflow betas. Relatedly, Gormsen and Koijen (2020) also use a fundamentals-based asset-pricing model along with dividend futures to isolate a large impact of COVID-19 via the earnings growth channel but do not link as we do asset pricing to stochastic transmission shocks.

Finally, while vaccines that are expected to arrive in a couple of years have little influence on conditional distribution of infections in short-run, they matter greatly, along with transmission volatility, for firm valuations nonetheless since markets are forward looking — discounting cashflow damage from COVID-19 far into the future. Even slight changes in vaccine arrival rates have large implications for valuations.

In short, our paper's contribution is to demonstrate how an analysis of pandemics fundamentally differs when using a stochastic epidemic model as opposed to relying on deterministic models and the $\mathcal{R}_0$ heuristic as an approximation. Our stochastic epidemic model can be used for further analysis such as stochastic control of pandemics or endogenizing the arrival of vaccines, which we leave for future research.

Our paper proceeds as follows. We present our epidemic model in Section 2 and the valuation model in Section 3. We describe our data in Section 4. We explain our calibration, estimation and forecast procedures in Section 5. In Section 6, we characterize the risk of our epidemic process by studying the analytical conditional distribution of I_t. In Section 7, we highlight the role of stochastic transmission shocks and vaccine arrival for COVID-19's damage to stock valuations. We conclude in Section 8.

2 Stochastic Epidemic Model

In this section, for pedagogical purposes, we construct our stochastic model by starting with the classic Kermack and McKendrick (1927) model. Time is continuous and the horizon is infinite. We normalize the total population size to one and there is no birth nor death in the population. As a key motivation is to design a tractable and parsimonious model to conduct risk management applications, we only model two compartments (groups): infected

and infectious (I) and susceptible (S) (or equivalently uninfected).[10] Within each group, the population is homogeneous and well mixed. Let I_t and S_t denote the mass of the infected population and the susceptible at time t, respectively. As $I_t + S_t = 1$ at all t, we only need to keep track of the evolution for I_t, which is the single state variable in our model.

2.1 Deterministic SIS Model

Transmission rate in classic SIS setting. How does the disease get transmitted from an infected to a susceptible? The probability that an infectious individual meets a susceptible is proportional to the product of their population mass, $I_t(1-I_t)$, with an effective transmission rate, which we denote by β. Thus over the interval $[t, t+dt)$ the total number of new infections is

$$\beta I_t S_t dt = \beta I_t(1 - I_t)dt\,.$$

The infected recovers and becomes susceptible in our model. Let $\gamma > 0$ denote the rate at which an infected recovers. Hence, $1/\gamma$ is the duration for an infected to be infective. Subtracting the mass for the recovered $\gamma I_t dt$ over the interval $[t, t+dt)$ from the newly infected $\beta I_t(1 - I_t)dt$, we obtain the following process for dI_t, the net change of I_t:

$$dI_t = \beta I_t(1 - I_t)dt - \gamma I_t dt\,. \tag{1}$$

The solution of (1) satisfies the following logistic function:[11]

$$I_t = \left[\frac{\beta}{\beta - \gamma}\left(1 - e^{-(\beta-\gamma)t}\right) + \frac{1}{I_0}e^{-(\beta-\gamma)t}\right]^{-1}\,. \tag{2}$$

Basic reproduction number $\mathcal{R}_0$. Next, we introduce the basic reproduction number $\mathcal{R}_0$, which is defined as the expected number of secondary infections generated by a single (representative) infected individual in a completely susceptible population:

$$\mathcal{R}_0 = \frac{\beta}{\gamma}\,. \tag{3}$$

[10] In the epidemiology literature, there are various generalized formulations of these compartmental models. Widely used ones include SIR (susceptible, infected, recovered) and SEIR (susceptible, exposed, infected, and recovered) models. See Andersson and Britton (2012) and Brauer, Driessche and Wu (2008) for textbook treatments.

[11] If $\beta = \gamma$, by applying the L'hopital's rule to (2), we obtain $I_t = \left(\beta t + \frac{1}{I_0}\right)^{-1}$.

If $\mathcal{R}_0 \leq 1$ (when $\beta \leq \gamma$), the disease eventually is extinct, as (2) implies $\lim_{t\to\infty} I_t = 0$. If $\mathcal{R}_0 > 1$, the infected population I_t reaches the maximum level, $I_\infty = 1 - \mathcal{R}_0^{-1}$ as $t \to \infty$ provided that $I_0 \neq 1 - \mathcal{R}_0^{-1}$.

We will use the term basic reproduction number and reproduction number interchangeably. The literature sometimes refers to the effective reproduction number at time t, which is the basic reproduction number multiplied by the susceptible mass. The effective reproduction number $\mathcal{R}_0\,(1 - I_t)$ is time-varying in classic deterministic models.

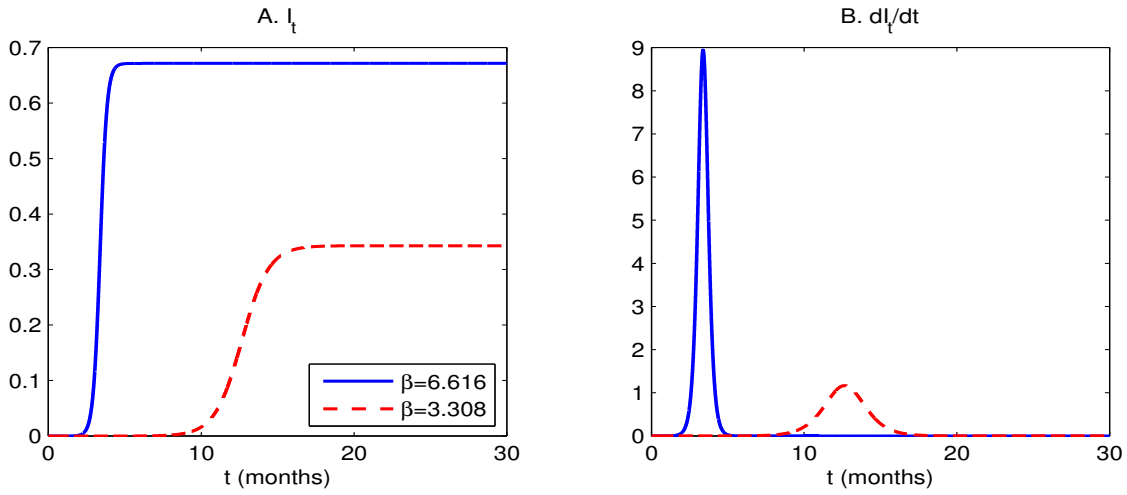

Figure 1: The infected fraction (I_t) and the net change (dI_t/dt) in deterministic SIS model with $I_0 = 2 \times 10^{-7}$ based on the US data as of March 1st and $\gamma = 2.173$ per month.

Deterministic infection forecasts. In Figure 1, we plot the infected mass I_t at t in Panel A and the net change of the infected mass dI_t/dt in Panel B with the initial value of $I_0 = 66/(3.28 \times 10^8) = 2 \times 10^{-7}$ (as there were 66 infective individuals on March 1st in the US and the US population as of 2019 is 328 million.) The solid blue lines correspond to the solution for our deterministic case using our estimate of the transmission rate for COVID-19 that we discuss in Section 5. By reducing β by half from 6.616 to 3.308 per month, such as using economy-wide lockdowns, we lower the basic reproduction number $\mathcal{R}_0$ by half from 3.045 to 1.522 (unlike the three structural parameters, $\mathcal{R}_0$ is invariant to the time horizon we choose). As a result, the eventual infected fraction, I_∞, decreases by half from 67.1% to

34.3% of the entire population.

Panel B captures the widely discussed flattening the curve argument (see, e.g., Atkeson (2020) and Gourinchas (2020)). Here, the curve refers to the net change of the infected population, dI_t/dt, as a function of time t. If the government successfully reduces β by half via social distancing and other interventions, this deterministic evolution curve is indeed significantly flattened and postponed. Specifically, this curve peaks at a bit over one year ($t = 12.657$ months) if $\beta = 3.308$ rather than at a bit over one quarter ($t = 3.384$ months). The curve of the net change, dI_t/dt, is substantially flattened.

Note the very sharp increase of I_t at the very early stage. This is because early on I_t is close to zero and we can thus effectively drop the $(1 - I_t)$ terms and approximate I_t as an exponential process: $dI_t \approx (\beta - \gamma) I_t \, dt$ with the approximate solution: $I_t \approx I_0 e^{(\beta-\gamma)t}$.

Obviously, exponential growth at a large rate $\beta - \gamma$ is incompatible with convergence of I_t to $I_\infty = 1 - \mathcal{R}_0^{-1}$ as $t \to \infty$. This is due to the dampening effect of I_t on its own growth. As the fraction of the infected increases, fewer are susceptible, which lowers dI_t/I_t. That is, the higher the level of I, the lower the infection growth rate dI_t/I_t.

2.2 Stochastic SIS Model

Aggregate transmission rate shock. A simple way to model stochastic transmission is to replace the constant rate β with a stochastic rate, which we denote by $\widetilde{\beta}$. For expositional purposes, consider a discrete-time setting. The simplest choice for a stochastic $\widetilde{\beta}$ is an independently and identically distributed (i.i.d.) random variable. Fix a small time increment Δ, we write

$$\widetilde{\beta}_t \, \Delta = \beta \Delta + \sigma \sqrt{\Delta} \, \epsilon_t \,, \tag{4}$$

where both β and σ are constant parameters and ϵ_t is a mean-zero standard normal random variable.[12] Mapping (4) into our continuous-time formulation, we obtain

$$\widetilde{\beta}_t \, dt = \beta dt + \sigma d\mathcal{Z}_t \,, \tag{5}$$

[12]By assuming ϵ_t is i.i.d., we make the transmission rate $\widetilde{\beta}_t$ stochastic but without introducing an additional state variable for the transmission rate. We leave generalizations of our model to allow for a richer specification of $\widetilde{\beta}_t$ for future work.

where $\mathcal{Z}_t$ is a standard Brownian motion.

By using $\widetilde{\beta}\,dt$ given in (5) to replace βdt in (1) and then combining drift and diffusion terms, we obtain the following stochastic differential equation (SDE) for I_t:

$$dI_t = [\beta(1 - I_t) - \gamma]\, I_t\, dt + \sigma\, I_t(1 - I_t)\, d\mathcal{Z}_t\,. \tag{6}$$

The drift term is the same as in the deterministic SIS model, while the diffusion term captures the uncertainty of the epidemiological evolution process. When no one is infected ($I_t = 0$), the disease is extinct: $dI_t = 0$ as both drift and volatility terms in (6) are zero. If the entire population is infected ($I_t = 1$), the volatility has to be zero and the drift has to be negative so that the model is well posed.[13] Unlike $I_t = 0$, $I_t = 1$ is not an absorbing state as $\gamma > 0$.

Note that both the drift and volatility of the growth rate for the infected population, dI/I, depend on $(1 - I)$, the population of the susceptible. Specifically, the higher the level of I, the lower the drift (i.e., the expected infection growth rate) of dI_t/I_t. As the fraction of the infected increases, fewer are susceptible, which dampens the drift of dI/I.

To complete the description of our compartmental model, below we report the dynamics for the susceptible population S_t:

$$dS_t = (\gamma - \beta S_t)\, I_t\, dt - \sigma\, S_t I_t\, d\mathcal{Z}_t\,. \tag{7}$$

Permanence of initial transmission shocks. The process for I_t given in (6) is not a Geometric Brownian motion (GBM) process widely used in Economics and Finance. But at a very early stage, I_t is close to zero; therefore, we can effectively drop the $(1 - I_t)$ terms in both drift and volatility functions and approximate I_t via a GBM process: $dI_t \approx (\beta - \gamma) I_t\, dt + \sigma\, I_t\, d\mathcal{Z}_t$. That is, in the early stage, I_t evolves as

$$I_t \approx I_0 \exp\left[\left(\beta - \gamma - \frac{\sigma^2}{2}\right) t + \sigma \mathcal{Z}_t\right] = I_0 e^{(\mathcal{R}_0 - 1)\gamma t} \exp\left(-\frac{\sigma^2}{2} t + \sigma \mathcal{Z}_t\right)\,. \tag{8}$$

Unlike the exponential growth approximation for I_t in the deterministic model, in our stochastic model, I_t is not only driven by $\mathcal{R}_0$ but also by the (exponential) martingale,

[13] If volatility is not zero or drift is positive at $I_t = 1$, the probability that I_t exceeds one is strictly positive, inconsistent with our model's assumption that the total population is normalized to one.

the second exponential term in (8). This second term is equally important in driving the dynamics of I_t as the first (exponential) term involving $\mathcal{R}_0$.

Because very few are infective early on, the change of I_t is highly idiosyncratic as the diffusion term dominates the drift term. A few super-spreader events early on have outsized permanent effects on the evolution of I_t. On the other hand, if there are few such events early on, then the total infected population stays low for an extended period of time causing the disease to be not that damaging. That is, in the very early stage, it is the sequence of realized values of $\widetilde{\beta}$, not the expected transmission rate β used in the deterministic compartmental epidemic models, driving how fast the disease spreads.

Epidemiologists also use networks and branching processes to model the disease spread, especially at the early stage. These network-based models confirm our intuition described above. Depending on the network structure and the network position of the first few infective, the disease could turn out to be either superspreading or extinct. See Newman (2018) for a textbook discussion on how network-based epidemiological models naturally generate stochastic transmission rates.

While the leading epidemiological models have rich compartmental specifications for agents and recognize the extreme difficulty of estimating $\mathcal{R}_0$ especially at the very beginning of a disease outbreak, we are among the first to emphasize the quantitative importance of volatility σ on the stochastic transition dynamics of I_t, which in turn has important implications on policy recommendations on how to efficiently manage epidemic risk.

Three-parameter non-linear diffusion process. We have generalized a two-parameter (β and γ) deterministic SIS model to a three-parameter (β, γ, and σ) non-linear diffusion process.

By applying Ito's Lemma to (6), we obtain:

$$d \ln I_t = q(I_t)dt + (1 - I_t)\sigma \, d\mathcal{Z}_t \,, \tag{9}$$

where the drift for $\ln I_t$ is a quadratic function in I_t:

$$q(I) = \beta(1 - I) - \frac{\sigma^2}{2}(1 - I)^2 - \gamma \,. \tag{10}$$

Equations (9)-(10) are convenient to work with when we analyze the stationary distribution.

Unlike in the deterministic model, which generates a single number for I_t at any t, in order to fully capture the disease transmission dynamics, we next characterize the time-0 conditional distribution of I_t for all t. Let $f(I_t, t; I_0)$ denote the time-0 conditional density function for I_t, the infected mass at t given the initial infected mass I_0.

Conditional distribution. The density function, $f(I,t)$, satisfies the following Kolmogorov forward equation:

$$0 = \frac{\partial f(I,t)}{\partial t} + \frac{\partial \left[(\beta(1-I)-\gamma)If(I,t)\right]}{\partial I} - \frac{1}{2}\frac{\partial^2 \left[(\sigma I(1-I))^2 f(I,t)\right]}{\partial I^2}\,. \tag{11}$$

The first term is the time effect on $f(I,t)$, the second term is the drift effect on $f(I,t)$, and the last term is the volatility effect on $f(I,t)$. In Section 6, we show how uncertainty substantially alters the transmission dynamics.

Next, we incorporate the impact of stochastic vaccine arrival.

2.3 Stochastic Vaccine Arrival

We assume that COVID-19 will disappear following a successful vaccine development.[14] Specifically, we use the following SDE to model the evolution of I_t:

$$dI_t = \left[\beta(1-I_{t-}) - \gamma\right] I_{t-}\, dt + \sigma\, I_{t-}(1-I_{t-})\, d\mathcal{Z}_t - I_{t-} d\mathcal{J}_t\,. \tag{12}$$

We capture this vaccine arrival effect on I_t via the third term, where $\mathcal{J}_t$ is a (pure) jump process with a constant arrival rate, which we denote by λ. When a vaccine is successfully developed, i.e., $d\mathcal{J}_t = 1$, the pandemic is extinct. We can generalize our model to allow for a multiple-stage vaccine development process with a gradual reduction of the infected population without losing much analytical tractability.[15]

[14] The assumption that vaccine takes effect immediately is clearly made for simplicity. In reality, it may take a while for the population to be vaccinated and not everyone will be vaccinated. We can generalize our vaccine model to allow for a (large) fraction of the population to be vaccinated leaving a (small) fraction still susceptible (at the cost of additional complexity.) But the core of our analysis will remain valid.

[15] For brevity, we leave this extension out.

3 Modeling COVID-19 Damage to Valuations

In this section, we develop a parsimonious yet operational model to capture the impact of pandemic shocks on fundamentals-based valuation. We show how COVID-19 parameters β (equivalently $\mathcal{R}_0$) and σ together with asset-pricing specifications impact valuation. The purpose of our analysis to compare the financial impact of infection forecasts generated from a deterministic versus a stochastic epidemic model of COVID-19 through the lens of a dynamic asset-pricing model.

In Section 3.1, we propose a valuation model before unanticipated pandemic arrival. In Section 3.2, we propose a valuation model after unanticipated pandemic arrival and no expectation of vaccine down the road. In Section 3.3, we incorporate stochastic vaccine arrival into the pricing model of Section 3.2.

3.1 Valuation Before Unanticipated Pandemic Arrival

To ease our exposition and set up the basic apparatus into which we later incorporate COVID-19 shocks, we first introduce a simple asset-pricing framework with no pandemic shocks, i.e., under normal business-as-usual environment or when $I_t = 0$. We start with the following widely-used simple stochastic discount factor (SDF), $\mathbb{M}_t$, in the normal times:[16]

$$\frac{d\mathbb{M}_t}{\mathbb{M}_t} = -r\,dt - \eta^{\mathcal{B}}\,d\mathcal{B}_t\,, \tag{13}$$

where $\mathcal{B}_t$ is the standard Brownian motion for the aggregate shock.[17] Here, r is the risk-free rate and $\eta^{\mathcal{B}}$ is the market price of risk for the aggregate shock. For simplicity, let r and $\eta^{\mathcal{B}}$ be constant. Equation (13) implies a one-factor model where the factor can be the aggregate consumption growth shock as in Lucas-style representative-agent general-equilibrium models or the market portfolio return in Sharpe (1964) CAPM and Merton-Samuelson's portfolio choice problem. Here, $\eta^{\mathcal{B}}$ is positive as a positive shock $d\mathcal{B}_t$ to the aggregate consumption growth or market return is good news which lowers the investor's marginal utility or equivalently $\mathbb{M}_t$.

[16] This is the SDF in Black and Scholes (1973), Merton (1973), and Lucas (1978), among other models. See Duffie (2001) and Cochrane (2009) for textbook treatments.

[17] No arbitrage requires that the drift of $\mathbb{M}_t$ is equal to the minus interest rate, $-r$.

Next, we turn to the cash-flow (earnings) process Y_t for the asset. As in the literature, we assume that Y_t follows a geometric Brownian motion (GBM) process:

$$\frac{dY_t}{Y_t} = g_0 dt + \rho\phi \, d\mathcal{B}_t + \sqrt{1-\rho^2}\,\phi \, d\mathcal{W}_t \,, \tag{14}$$

where $\mathcal{B}_t$ is the aggregate shock introduced in (13) and $\mathcal{W}_t$ is the standard Brownian motion driving the idiosyncratic earnings risk. By construction, $\mathcal{B}_t$ and $\mathcal{W}_t$ are orthogonal. In (14), g_0 is the expected earnings growth (drift), ϕ is the volatility of earnings growth, which includes the aggregate component $\rho\phi$ and the idiosyncratic component $\sqrt{1-\rho^2}\,\phi$. That is, ρ is the correlation coefficient between the aggregate shock $\mathcal{B}_t$ and the asset's earnings process. For simplicity, we let g_0, ϕ, and ρ all be constant.

Let P denote the asset's value. The standard asset-pricing equation holds (Duffie, 2001):

$$P_t = \mathbb{E}_t \left(\int_t^\infty \frac{\mathbb{M}_s}{\mathbb{M}_t} Y_s \, ds \right) . \tag{15}$$

In Appendix C, using (13) and (14) and solving (15), we show that the asset's value is proportional to its earnings, $P_t = p_0 Y_t$, where the price-earnings ratio, p_0, is a constant:

$$p_0 \;\; = \;\; \frac{1}{r + \rho\phi\eta^{\mathcal{B}} - g_0} \,. \tag{16}$$

Equation (16) is the well-known Gordon growth model where $\left(r + \rho\phi\eta^{\mathcal{B}}\right)$ is the asset's constant cost of capital (discount rate) and g_0 is the earnings growth rate. This asset earns a risk premium of $\rho\phi\eta^{\mathcal{B}}$, which is given by the the product of the market price of risk $\eta^{\mathcal{B}}$ and $\rho\phi$, the systematic volatility component of ϕ and consistent with the one implied by the widely used CAPM.[18]

3.2 Valuation After Pandemic Arrival and with no Vaccine

Next, we incorporate pandemic shocks into our pricing model. As COVID-19 is clearly an aggregate shock, it changes the equilibrium SDF. To highlight the role of aggregate stochastic

[18] In Black and Scholes (1973), Merton (1973), and Lucas (1978), $\eta^{\mathcal{B}}$ is the ratio between the (expected) excess stock market return, $r_m - r$, divided by the market portfolio return volatility, σ_m, i.e., $\eta^{\mathcal{B}} = (r_m - r)/\sigma_m$. Therefore, CAPM holds here and the asset's CAPM beta, β_A, is equal to $\rho\phi/\sigma_m$ and the asset's excess return is thus $\beta_A(r_m - r) = \rho\phi(r_m - r)/\sigma_m = \rho\phi\eta^{\mathcal{B}}$, as $\eta^{\mathcal{B}} = (r_m - r)/\sigma_m$.

transmission shocks, we assume that at both the micro and the aggregate levels, parameters for the business-as-usual aggregate variables and idiosyncratic risks, e.g., market price of business-as-usual risk $\eta^{\mathcal{B}}$, the risk-free rate r, the asset's idiosyncratic volatility $\sqrt{1-\rho^2}\phi$ and its business-as-usual volatility $\rho\phi$, do not change with the unexpected pandemic arrival. We can of course also allow the business-as-usual parameters to also change as well without any technical difficulties.

SDF. We generalize the SDF by incorporating pandemic shocks into $\mathbb{M}_t$ given in (13):

$$\frac{d\mathbb{M}_t}{\mathbb{M}_t} = -r dt - \eta^{\mathcal{Z}}\, d\mathcal{Z}_t - \eta^{\mathcal{B}}\, d\mathcal{B}_t\,. \tag{17}$$

As a positive pandemic shock $d\mathcal{Z}_t$ (which increases I) is bad news for the aggregate economy, the marginal utility of the investor (and hence the SDF $\mathbb{M}_t$) should increase with I_t, which means $\eta^{\mathcal{Z}} < 0$, in contrast to a positive $\eta^{\mathcal{B}}$ for the business-as-usual aggregate shock.

At the micro level, pandemic may change both an asset's cash-flow and discount-rate processes. Some assets, e.g., airline assets, are more exposed to pandemics than others.

Asset's earnings process. We generalize the earnings model in normal times given in (14) to incorporate the impact of pandemic on earnings as follows:

$$\frac{dY_t}{Y_t} = g(I_t)dt + v(I_t)\, d\mathcal{Z}_t + \rho\phi\, d\mathcal{B}_t + \sqrt{1-\rho^2}\,\phi\, d\mathcal{W}_t\,. \tag{18}$$

Pandemic shocks have two direct effects on earnings: 1) it changes the growth rate forecast from g_0 to $g(I_t)$; and 2) it may also expose earnings to additional volatility, captured by the function $v(I_t)$, which measures the earnings risk exposure to the pandemic shock $d\mathcal{Z}_t$. For airline companies, the earnings growth is negatively impacted by I_t: $g(I_t) \leq g_0$ and $g'(I_t) \leq 0$. Additionally, the earnings volatility function (the loading on the pandemic shock $\mathcal{B}_t$) may also be negative ($v(I_t) \leq 0$), because an unexpected increase of I_t may lower earnings growth dY_t/Y_t.

Generalized equity valuation (Gordon growth) model. Because of the geometric feature of the earnings process, the asset's value is proportional to its earnings Y_t:

$$P_t = P(Y_t, I_t) = p(I_t)Y_t\,, \tag{19}$$

where $p(I_t)$ is the equilibrium price-earnings ratio. In Appendix C, we show that $p(I)$ solves the following valuation equation:

$$\begin{aligned}\left[\left(r + \rho\phi\eta^{\mathcal{B}} + v(I)\eta^{\mathcal{Z}}\right) - g(I)\right] p(I) &= 1 + \left[\beta^{\mathbb{Q}}(1-I) - \gamma\right] Ip'(I) \\ &\quad + v(I)\sigma(1-I)Ip'(I) + \frac{(\sigma I(1-I))^2}{2}p''(I)\,, \end{aligned} \tag{20}$$

where $\beta^{\mathbb{Q}}$ is the (risk-adjusted) transmission rate (i.e., under the risk-neutral measure $\mathbb{Q}$):

$$\beta^{\mathbb{Q}} = \beta - \eta^{\mathcal{Z}}\sigma\,. \tag{21}$$

The pricing equation (20) reveals that stochastic transmission rates generate the following several effects on the valuation ratio $p(I)$. First, volatility induces a *convexity effect* on valuation $p(I)$, which is captured by the last term on the right side of (20). Second, COVID-19 changes the earnings expected growth rate $g(I)$.

Finally, being an aggregate shock, COVID-19 has rich implications on the asset's risk premium. Specifically, there are three risk-premium channels. First, the risk-adjusted transmission rate, $\beta^{\mathbb{Q}}$, is larger than β (Recall that $\eta^{\mathcal{Z}} < 0$ as a pandemic shock increasing I_t is bad news for the representative agent.) Put simply, for valuation purposes, for a fixed value of transmission rate β, Wall Street should use a higher transmission rate $\beta^{\mathbb{Q}}$ to account for the fact that the pandemic shock is an aggregate shock.

Second, the covariance between the asset's pandemic-specific risk exposure and the pandemic component of the SDF generates an instantaneous pandemic risk premium term $v(I)\eta^{\mathcal{Z}}$ on the left side of (20). Third, the instantaneous covariance between earnings volatility and I also contributes to the risk premium, captured by the third term on the right side of (20).

When $I = 0$, we expect to uncover our solution under normal times as $I = 0$ is an absorbing state in our stochastic SIS model.[19] We show that

$$p(0) = p_0\,, \tag{22}$$

[19]To be consistent with our pricing in normal times, we set $g(0) = g_0$ and $v(0) = 0$.

where p_0 is given in (16). Turning to the other boundary when everyone is infected ($I = 1$). The ODE (20) is simplified as follows:

$$\left[r - g(1) + v(1)\eta^{\mathcal{Z}} + \rho\phi\eta^{\mathcal{B}}\right] p(1) = 1 - \gamma p'(1)\,. \tag{23}$$

Unlike $I = 0$, $I = 1$ is not an absorbing state as the recovery rate $\gamma > 0$. The term, $-\gamma p'(1)$ on the right side of (23), reflects the effect of recovery on valuation.

In summary, the generalized (Gordon growth) equity valuation model for the price-earnings ratio, $p(I)$, over $[0, 1]$ is characterized by the ODE pricing equation (20) together with boundary conditions (22)-(23).

Next, we incorporate the effect of vaccine arrival on valuation. A successful vaccine development will significantly influence both corporate earnings and the pricing of the aggregate pandemic shock.

3.3 Pricing with Stochastic Vaccine Arrival

To capture the impact of vaccine arrival on the earnings process, we generalize (18) as:

$$\frac{dY_t}{Y_{t-}} = g(I_{t-})dt + v(I_{t-})\,d\mathcal{Z}_t + \rho\phi\,d\mathcal{B}_t + \sqrt{1-\rho^2}\,\phi\,d\mathcal{W}_t + \left(e^{n(I_{t-})} - 1\right) d\mathcal{J}_t\,, \tag{24}$$

where $n(I_{t-})$ is the instantaneous logarithmic change of earnings from the pre-jump to the post-jump level conditional on the vaccine arrival, i.e., $n(I_{t-}) = \ln(Y_t/Y_{t-})$, if $d\mathcal{J}_t = 1$.

News about vaccine development is an aggregate shock and thus risk-averse investors demand a risk premium for the stochastic timing of vaccine arrival. Specifically, we incorporate vaccine arrival timing risk into our pricing model by generalizing the SDF $\mathbb{M}_t$ for normal times given in (17) as follows:

$$\frac{d\mathbb{M}_t}{\mathbb{M}_{t-}} = -r dt - \eta^{\mathcal{Z}}\,d\mathcal{Z}_t - \eta^{\mathcal{B}}\,d\mathcal{B}_t - (1 - e^{\kappa})\,(d\mathcal{J}_t - \lambda dt)\,, \tag{25}$$

where the last term captures the effect of stochastic vaccine arrival on the SDF and it is a martingale under the physical measure as the drift rate of $\mathbb{M}_t$ is equal to the negative interest rate by no arbitrage (Duffie, 2001). Upon the successful vaccine development at t, i.e., $d\mathcal{J}_t = 1$, the SDF immediately changes from $\mathbb{M}_{t-}$ by $\mathbb{M}_t = e^{\kappa}\,\mathbb{M}_{t-}$. As vaccine arrival

is good news, investors' marginal utility (SDF) is lower after vaccine arrival and the market price of vaccine arrival risk is negative, i.e., $\kappa < 0$.

Absent a vaccine, the pandemic persists and its distribution converges to its stationary distribution. Therefore, it may have long-lasting effects on the economy. But a potential vaccine effectively truncates the duration of the pandemic and limits the impact of pandemic shocks up to the moment of vaccine arrival hence making the effect of pandemic shock transitory.

In Appendix C, we obtain the following ODE for $p(I)$:

$$\begin{aligned}\left[\left(r+\rho\phi\eta^{\mathcal{B}}+v(I)\eta^{\mathcal{Z}}\right)-g(I)+\lambda^{\mathbb{Q}}\right]p(I) &= 1+\lambda^{\mathbb{Q}}e^{n(I)}p_0+\left[\beta^{\mathbb{Q}}(1-I)-\gamma\right]Ip'(I) \\ &\quad +v(I)\sigma(1-I)Ip'(I)+\frac{(\sigma I(1-I))^2}{2}p''(I)\,,\end{aligned} \tag{26}$$

where $\beta^{\mathbb{Q}}=\beta-\eta^{\mathcal{Z}}\sigma$ is the risk-adjusted disease transmission rate given in (21) and $\lambda^{\mathbb{Q}}$ is the risk-adjusted vaccine arrival rate:

$$\lambda^{\mathbb{Q}}=\lambda e^{\kappa}\,. \tag{27}$$

As investors demand a risk premium for the uncertain vaccine arrival timing, the market price of vaccine arrival risk is negative, $\kappa < 0$. That is, in equilibrium, the vaccine arrives at a lower rate under the risk-neutral measure $\mathbb{Q}$, than the rate under the physical measure: $\lambda^{\mathbb{Q}} < \lambda$ (Duffie, 2001).

Vaccine arrival brings two new terms into the pricing equation (20) for the case with no possibility of vaccine. The term $\lambda^{\mathbb{Q}}e^{n(I)}p_0$ on the right side of (26) accounts for the anticipated significant stock market revaluation upon a successful vaccine development. It is equal to the product of risk-adjusted probability for vaccine arrival per unit of time, $\lambda^{\mathbb{Q}}$, and the size of valuation revision $e^{n(I)}p_0$. (The multiple $e^{n(I)}$ reflects the discrete jump of earnings upon vaccine arrival, e.g., an instantaneous jump of consumer demand for air travel.) The other new term is $\lambda^{\mathbb{Q}}$ on the left side of (26), which recognizes the eventual extinction of the disease by elevating the discount rate by the risk-adjusted arrival rate of vaccine. The possibility of vaccine arrival makes the valuation problem much less sensitive to the pandemic process I_t.

4 COVID-19 Data

Our data on COVID-19 cases comes from COVID-19 Data Repository by Johns Hopkins available on github. The data keeps track of confirmed new cases, deaths, recoveries each day starting from January 22nd, 2020. The measure I_t in our model maps to the net number of outstanding infected cases at t, which is equal to the sum of the last period's I_{t-1} and the newly (reported) infected cases at t and subtracting deaths and recoveries, divided by the population of that country.

We follow leading epidemiological studies of COVID-19 and focus on China and countries (regions) that were at high risk due to air travel connected to China (Kucharski et.al. (2020)). There are a total of 16 countries in our sample. In Asia (Middle East), there are nine countries consisting of China, Japan, Malaysia, Singapore, South Korea, Taiwan (China), Thailand, United Arab Emirates and Vietnam. Among Western countries, these include Australia, Canada, France, Germany, Italy, United Kingdom, and United States.[20] While all these countries have significant air travel connections to China, they did not experience the same infection path. This is consistent with our model that each country experienced idiosyncratic paths (realizations) of transmission shocks at early stages.

In Figure 2, we plot the logarithmic growth rate $d\ln(I_t)$ for four countries of interest, China, Singapore, US and Italy. We can see that the epidemic curve of China reversed in the second half, while Singapore which has a fairly flat curve in the first half takes off in the second half. The same is true for Italy and the US. Again, most of the countries in our sample only started government lockdowns later in the second half of the sample and it takes time for these lockdowns to have an effect.

[20]Five of the original high-risk regions, Cambodia, India, Indonesia, Philippines and Russia, had no cases in January-February, so we exclude them from our analysis. These countries are thought to be the most problematic in terms of underreporting of cases. And we need some cases to estimate the model in the first place.

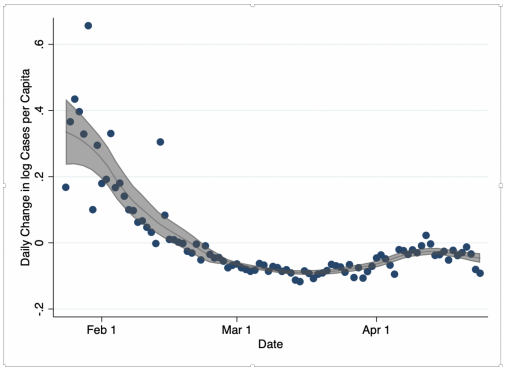

(a) China

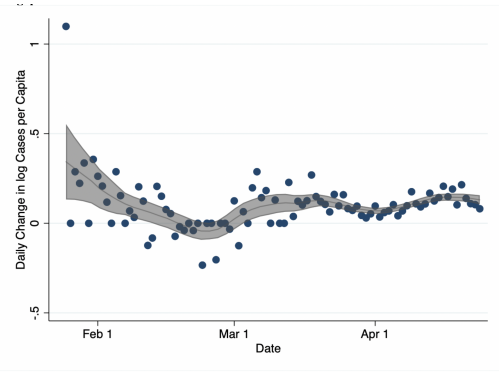

(b) Singapore

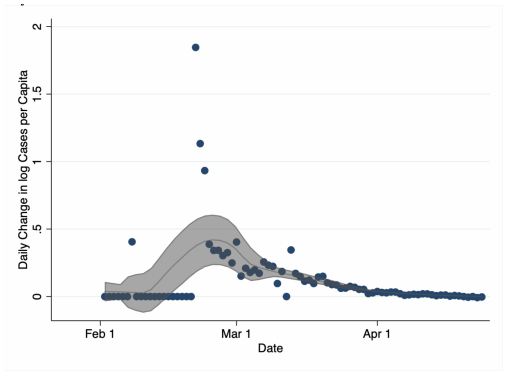

(c) Italy

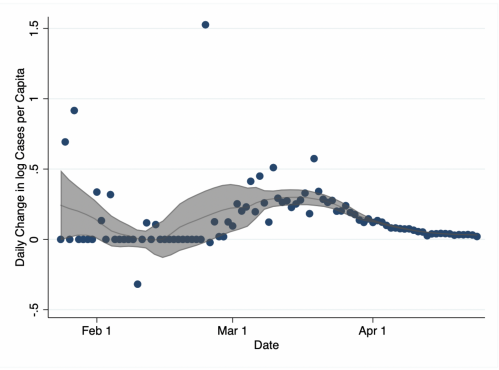

(d) US

Figure 2: Daily changes in $\ln I_t$, logarithmic infected population over time with shaded area beings the 95-percent confidence intervals.

5 Calibration, Estimation, and Forecasts

In this section, we fit our model to the data for the January-February period. Given the noisiness and short time series of the data, we do not attempt to capture the potential heterogeneity in models across regions. Rather we think it is appropriate to fit one model by pooling the 16 countries. We pursue a robust estimation strategy as follows. For each country, we can estimate β and σ using the brief time series. But we use as our estimate the mean of the values across the 16 regions weighted by the number of daily observations in each region. For instance, China has more observations in the first sub-period and will then get more weight in our estimate. We can then judge the sensibility of our estimates by comparing them to leading models of the early dynamics of COVID-19.

As we have pointed out a couple of times already, most governments only started inter-

vening in March. Hence, we view our estimates as representative of the underlying epidemic process or early COVID-19 dynamics absent government intervention.

Calibration of γ: Earlier epidemiological studies typically set γ by targeting the expected duration for an infected and infective individual to 14 days, which implies that the rate γ is equal to 1/14 per day, or $\gamma = 365/12/14 \approx 2.173$ per month. (Recall that in our convention, one period is one month.) Epidemiological studies typically view γ as highly predictable and relatively easy to estimate. They typically model this parameter as an Erlang distribution (Kucharski et.al. (2020)). By fixing γ, we leave out the impact of uncertainty of the exit rate on the disease spread.

Estimate of β: In Appendix A, we derive an OLS estimator for β given γ:

$$\widehat{\beta} = \frac{1}{N-1} \Sigma_{i=0}^{N-2} \frac{\frac{I_{i+1}}{I_i} - 1 + \gamma}{1 - I_i} \,. \tag{28}$$

Table 1 reports the distribution of the estimate across regions. We use the mean estimate from the January-February sample (6.616 per month) as our baseline estimate with a 95% CI of (2.443, 14.168).

Table 1: The percentiles and moments for the monthly estimates of parameters β and σ^2 with implied $\mathcal{R}_0$ based on the data during the period of January-February 2020.

	Percentiles					Moments	
Estimates	5%	25%	50%	75%	95%	Mean	Std. Dev.
β	2.443	4.191	6.332	8.246	14.168	6.616	3.242
σ^2	0.718	1.138	1.436	4.791	8.857	2.851	2.537
$\mathcal{R}_0$	1.124	1.928	2.915	3.795	6.521	3.045	1.493

Estimate of σ^2: In Appendix A, we show that the estimator for σ^2 is

$$\widehat{\sigma}^2 = \frac{\Sigma_{i=0}^{N-2} (\ln I_{i+1} - \ln I_i)^2}{\Sigma_{i=0}^{N-2} (1 - I_i)^2} \,. \tag{29}$$

Table 1 reports the distribution of the estimate across regions. We use the mean estimate of σ^2 from the January-February sample (2.851 per month) as our baseline estimate with a 90% CI of (0.718, 8.857). The implied estimate of σ is then $1.689 = \sqrt{2.851}$ per month.

Estimate of the basic reproduction number $\mathcal{R}_0$. Our estimate of the basic reproduction number $\mathcal{R}_0$, shown in Table 1, is $3.045 = 6.616/2.173$ with a 90% confidence interval of (1.12, 6.52) based on data from the period of January-February. As we have mentioned in the Introduction, our estimates are in line with leading studies.

Out-of-Sample Forecasts. In this section, we use the model estimated in the previous section to generate out-of-sample forecasts for March-April. For purposes of comparison to epidemiological studies' short-run forecasts, we set the vaccine arrival rate $\lambda = 0$ as our baseline since a vaccine is quite unlikely to arrive in the short term. In comparative statics below, we will then vary λ and see its effect on infection forecasts.

We can use our model to evaluate the effectiveness of government interventions in March and April. To the extent actual outcomes lie outside the 95% CI of our out-of-sample forecasts, we can reject our model presumably attributable to government intervention. In summary, our model is rejected for only two countries (China and South Korea) that have bent the curve. Most of the countries infected outcomes in March-April fit within the 95% CI of our model's conditional forecast even as there is evidence of flattening of the curves. But given the large conditional variances of out-of-sample forecasts, it is not possible to definitely reject the model for most countries.

To see this, among the nine regions in Asia and Middle East (Figure 3), Japan, Singapore, and Australia line up reasonably with our model projections. The exceptions are China and South Korea which have successfully bent the curve: China in March already appears to have broken out of the lower bound of the 95% CI followed by South Korea at the beginning of April.

We next turn to the seven western countries in Figure 4. For the US, our model does a reasonable job in early March and then later in April, but in the middle of this period,

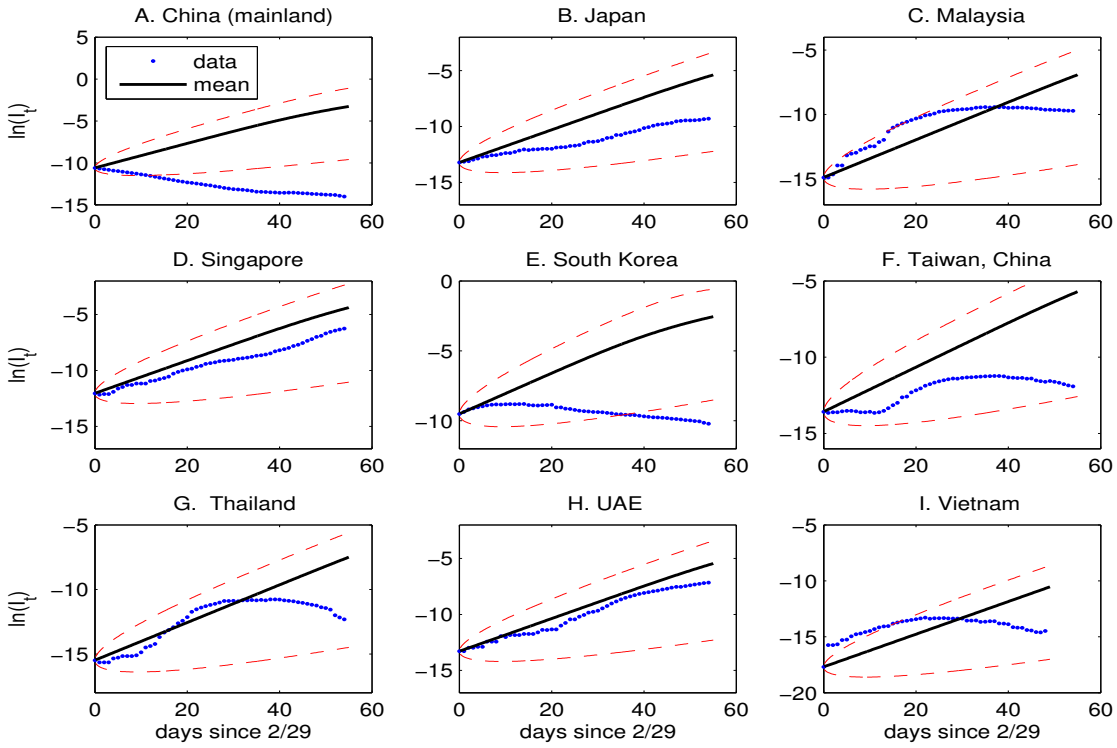

Figure 3: This figure plots the conditional forecast of $\ln I_t$ (means and 95% CIs) for Asian and Middle Eastern countries in our sample and compares them with March-April data. We use each region's data on March 1st to calculate its I_0 and use $\beta = 6.616$, $\gamma = 2.173$, $\sigma = 1.689$, and $\lambda = 0$ per month for their conditional distributions.

US cases are far above our 95-th percentile forecasts. But for many of the other Western countries, including surprisingly Italy, we see that their outcomes for the most part lie within our 95% CI. So overall, we view our intentionally parsimonious model as capturing some essential COVID-19 dynamics.

6 Conditional Distributions and Transition Dynamics of Infections

We now use our estimates from the previous section to calculate the conditional distribution of I_t via the Kolmogorov forward equation. We focus on estimates and outcomes for the US, though our discussion equally applies to the aforementioned regions in our out-of-sample forecast analyses. We compare these conditional forecasts to the solution for the deterministic

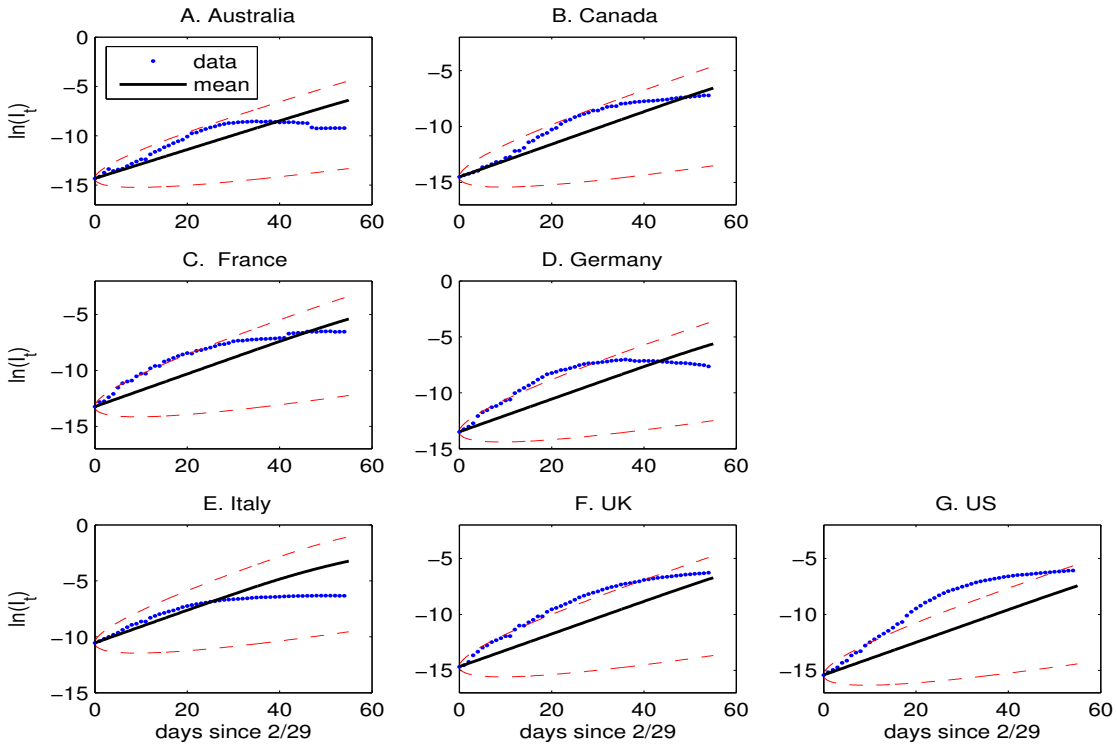

Figure 4: This figure plots the conditional forecast of $\ln I_t$ (means and 95% CIs) for Western countries in our sample and compares them with March-April data. We use each region's data on March 1st to calculate its I_0 and use $\beta = 6.616$, $\gamma = 2.173$, $\sigma = 1.689$, and $\lambda = 0$ per month for their conditional distributions.

SIS model ($\sigma = 0$) so as to draw implications regarding the usefulness of $\mathcal{R}_0$.

6.1 Stochastic SIS Model ($\sigma > 0$)

We now contrast the deterministic model projections with our stochastic model projections. In Table 2, we report the corresponding conditional means and variances for our stochastic SIS model with 1, 2, 4, 6, 8 weeks and 3, 4, 6, 9, 12 months time horizons.

As we stated in the Introduction, $\mathcal{R}_0$ mismeasures the benefits of lockdowns for two reasons. The first is the permanence of initial transmission shocks as we explained in deriving our model. The second reason is seen in this table. The conditional mean increases with the time horizon, as $\mathcal{R}_0 = 3.045$, which is significantly larger than one indicating a highly infectious and fast spreading disease. Note that at the very early stage, e.g., from 1 week

Table 2: Means and standard deviations of I_t over different time horizons conditional on $I_0 = 2 \times 10^{-7}$. This is our baseline case where parameter values are: $\beta = 6.616$, $\gamma = 2.173$, $\sigma = 1.689$, and $\lambda = 0$ per month with an implied value of $\mathcal{R}_0$, 3.045.

	Deterministic	Stochastic	
t	I_t	$\mathbb{E}(I_t)$	$\sqrt{\mathbb{V}ar(I_t)}$
1 wk	$5.6 * 10^{-7}$	$5.6 * 10^{-7}$	$5.4 * 10^{-7}$
2 wk	$1.6 * 10^{-6}$	$1.6 * 10^{-6}$	$2.6 * 10^{-6}$
4 wk	$1.2 * 10^{-5}$	$1.2 * 10^{-5}$	$4.3 * 10^{-5}$
6 wk	$9.3 * 10^{-5}$	$9.2 * 10^{-5}$	$6.0 * 10^{-4}$
8 wk	$7.1 * 10^{-4}$	$6.8 * 10^{-4}$	$5.2 * 10^{-3}$
3 mo	0.104	0.031	0.095
4 mo	0.630	0.165	0.235
6 mo	0.671	0.519	0.251
9 mo	0.671	0.636	0.151
12 mo	0.671	0.639	0.146
∞	0.671	0.639	0.144

up to 6-8 weeks, the conditional mean forecast of I in our stochastic model is essentially the same as in the deterministic model – this is because the stochastic exponential growth approximation works well when I_t is very low. Starting from 3 months, this approximation no longer works. Deterministic model infection forecasts based on $\mathcal{R}_0$ overshoot our model's conditional forecasts by a significant mount (0.104 for the deterministic model and 0.031 for our stochastic model). This is due to Jensen's inequality.

Furthermore, the conditional volatility is highly nonlinear and non-monotonic in the time horizon. For example, for the 3-month-ahead forecast, the monthly volatility of I_t (9.5%) is more than three times the mean (3.1%). Even with 6 months out, while the expected infected mass is 51.9% of the population, the two-standard-deviation bound for this estimate is still wide: from 27% to 77% of the population. The volatility declines once we go beyond 5 months out (Around 5 months, the volatility peaks at 0.287.) In other words, infection forecasts based on a deterministic model are poor approximations for the conditional forecasts of our model for a large range of periods.

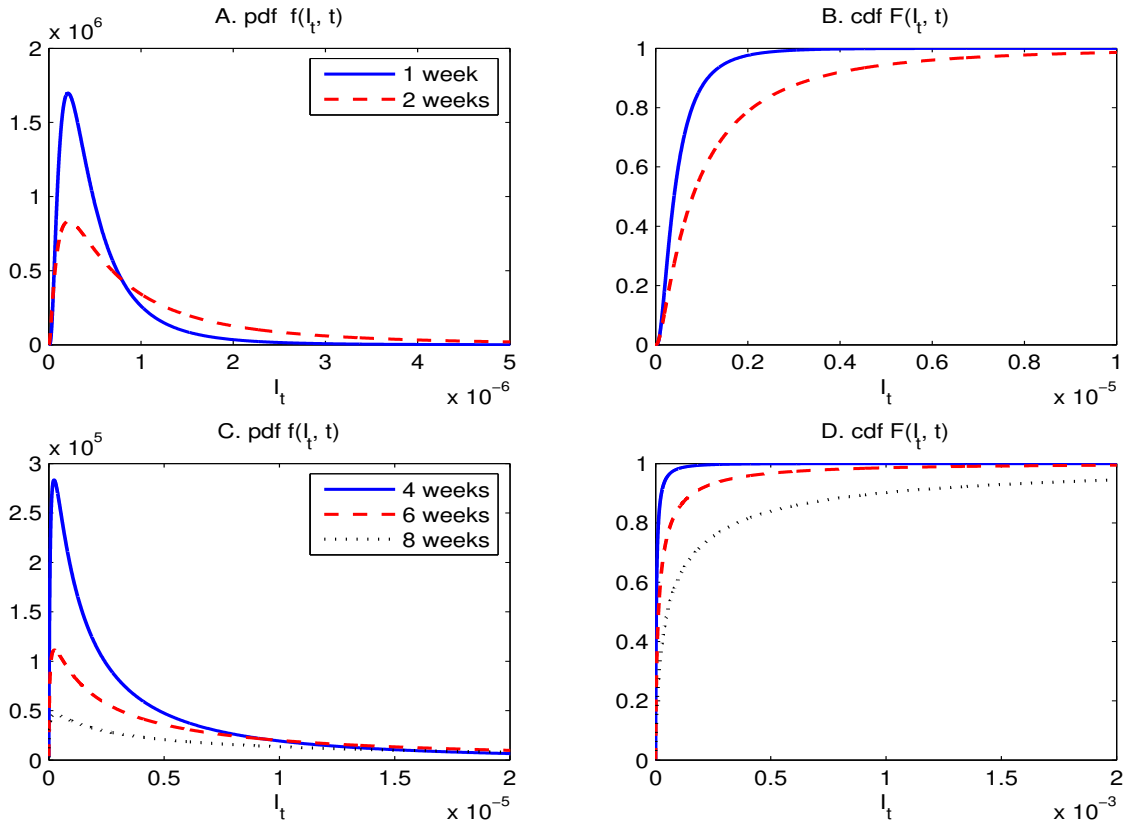

Figure 5: Conditional distributions of I_t in stochastic SIS model with $I_0 = 2 \times 10^{-7}$ based on the US data as of March 1st. The parameter values are $\beta = 6.616$, $\gamma = 2.173$, $\sigma = 1.689$, and $\lambda = 0$ per month.

In Figure 5, rather than simply reporting the conditional means and variances, we plot the conditional distributions of I_t with various time horizons: 1, 2, 4, 6 and 8 weeks (see Panels A and C for pdfs and Panels B and D for cdfs.) We plot the conditional distributions also with the initial value of $I_0 = 2 \times 10^{-7}$. Panel A shows that the conditional distribution for both one-week and two-week ahead are humped shaped. Panel B shows that the two-week-ahead distribution dominates the one-week-ahead distribution in the sense of first-order stochastic dominance (FOSD). For example, the one-week-ahead conditional probability that the infected mass exceeds 1×10^{-6} of the population is 12.9%, two-week-ahead probability (without intervention) significantly increases to 42.3%.

Panels C and D plot the conditional density and cumulative distribution functions respec-

tively for 4, 6 and 8 weeks out. We see continued shift of probability distributions to higher values of I as we increase the forecasting horizon. Indeed, the 8-week-ahead distribution dominates the 6-week-ahead distribution, which in turn dominates the 4-week-ahead distribution in the sense of FOSD. As an example, the probability that the infected mass (4-weeks ahead) exceeds 0.01% of the population is 1.7%, two and four extra weeks (without intervention) increase this probability to 15.1% and 38.6%, respectively. (Note the substantial scale change on the horizontal axis across panels in Figure 5.)

Stochastic Steady State (SS) and Stationary Distribution. Next we turn to the stochastic steady state and stationary distribution to gain some intuition for why $\mathcal{R}_0$ is an insufficient statistic for managing COVID-19 risks. The long-run distributional properties of the infected fraction I depend on all three parameters in a nonlinear way. Simply relying on $\mathcal{R}_0$, which is ratio between the expected transmission rate β and exit rate γ can be quite misleading.

It is useful to define the following variance-adjusted basic reproduction number:

$$\overline{\mathcal{R}}_0 = \frac{1}{\gamma}\left(\beta - \frac{\sigma^2}{2}\right). \tag{30}$$

Gray et al. (2011) show that whether $\overline{\mathcal{R}}_0$ exceeds one or not dictates the long-run convergence property of the model. There are two scenarios for the stationary distribution: 1) the persistence case where $\overline{\mathcal{R}}_0 > 1$: disease persists in the long run; 2) the extinction case where $\overline{\mathcal{R}}_0 \leq 1$: disease is extinct in the long run. That is, it is $\overline{\mathcal{R}}_0$, rather than $\mathcal{R}_0$ that describes whether the epidemic goes extinct in the long run.

While we have focused on how volatility σ significantly alters the pandemic transmission dynamics, it is also crucial for the long-run distribution of I. When $\overline{\mathcal{R}}_0 > 1$, there exists a unique stochastic SS at the level of $I_t = I^{SS}$, where I^{SS} is the unique positive root in $(0, 1)$ for the quadratic equation $q(I) = 0$ with $q(I)$ given in (10):

$$I^{SS} = \frac{1}{\sigma^2}\left[\sqrt{\beta^2 - 2\sigma^2\gamma} - \left(\beta - \sigma^2\right)\right]. \tag{31}$$

In this case, the infected mass I_t crosses its stochastic SS I^{SS} infinitely often with probability

one. The value of I^{SS} corresponds to the threshold of I to reach herd immunity in our stochastic SIS model.

In Figure 6, we plot the density function for the stationary distribution in Panel A and the quadratic equation for $q(I)$ in Panel B. For this case, $\overline{\mathcal{R}}_0 = 2.39 > 1$. As a result, there is a unique positive root $I^{SS} = 0.644$. The single mode of the stationary distribution is 0.723.

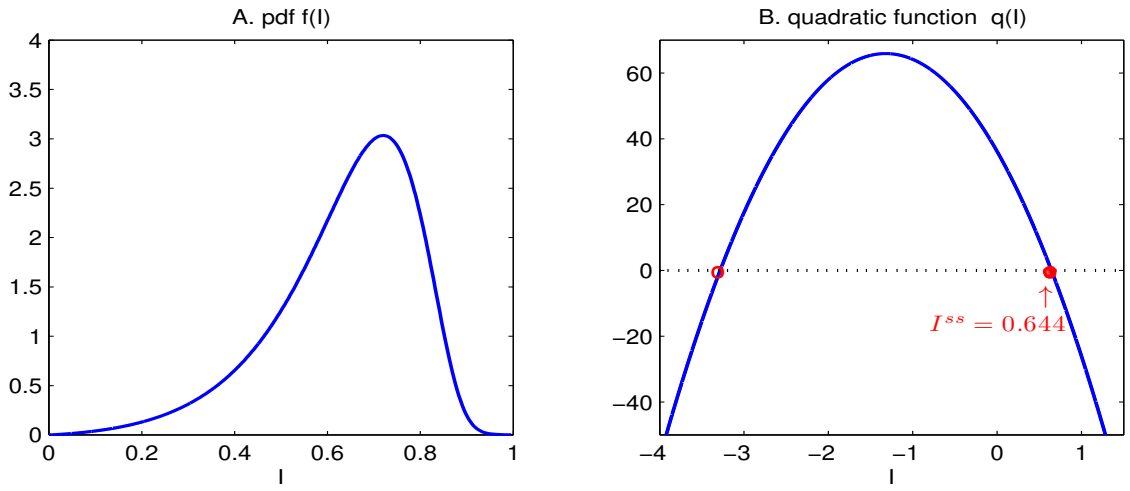

Figure 6: Panel A plots the stationary distribution of the infected population I for our baseline case. The mode of the distribution is 0.723. Panel B shows that there is a unique positive root, $I^{SS} = 0.644$, for $q(I) = 0$, the fundamental quadratic equation (10). Parameter values are $\beta = 6.616$, $\gamma = 2.173$, $\sigma = 1.689$, and $\lambda = 0$ per month.

6.2 Comparative Statics

Another way to see why $\mathcal{R}_0$ is an insufficient statistic to manage COVID-19 risks is to consider a comparative statics on β which directly maps to changes in $\mathcal{R}_0$. Discussions regarding government interventions have focused on keeping the reproduction number near one. But our comparative static calculations in Table 3 suggest that even at fairly high reproduction numbers the outbreak will likely be a slow burn.

Changing β or equivalently $\mathcal{R}_0$. Recall that when our baseline reproduction number is 3.045, our model predicts that at nine months out 63.6% of the US population will be infected with a conditional standard deviation of 15.1%. But reducing β and taking the reproduction

Table 3: Effects of Changing $\mathcal{R}_0$ on Conditional Distributions of I_t. The parameter values are: $\gamma = 2.173$, $\sigma = 1.689$, and $\lambda = 0$ per month. By definition, $\beta = \mathcal{R}_0\gamma$.

	A. $\mathcal{R}_0 = 2.75$			B. $\mathcal{R}_0 = 2.25$		
	Deterministic	Stochastic		Deterministic	Stochastic	
t	I_t	$\mathbb{E}(I_t)$	$\sqrt{\mathbb{V}ar(I_t)}$	I_t	$\mathbb{E}(I_t)$	$\sqrt{\mathbb{V}ar(I_t)}$
1 wk	$4.8 * 10^{-7}$	$4.8 * 10^{-7}$	$4.7 * 10^{-7}$	$3.8 * 10^{-7}$	$3.8 * 10^{-7}$	$3.6 * 10^{-7}$
2 wk	$1.2 * 10^{-6}$	$1.2 * 10^{-6}$	$1.9 * 10^{-6}$	$7.0 * 10^{-7}$	$7.0 * 10^{-7}$	$1.2 * 10^{-6}$
4 wk	$6.7 * 10^{-6}$	$6.7 * 10^{-6}$	$2.4 * 10^{-5}$	$2.5 * 10^{-6}$	$2.5 * 10^{-6}$	$8.8 * 10^{-6}$
6 wk	$3.8 * 10^{-5}$	$3.8 * 10^{-5}$	$2.6 * 10^{-4}$	$8.6 * 10^{-6}$	$8.6 * 10^{-6}$	$5.9 * 10^{-5}$
8 wk	$2.2 * 10^{-4}$	$2.2 * 10^{-4}$	$2.0 * 10^{-3}$	$3.0 * 10^{-5}$	$3.0 * 10^{-5}$	$3.5 * 10^{-4}$
3 mo	0.018	0.008	0.043	$6.9 * 10^{-4}$	$5.6 * 10^{-4}$	$7.2 * 10^{-3}$
4 mo	0.353	0.056	0.139	0.010	0.004	0.029
6 mo	0.636	0.302	0.282	0.451	0.038	0.117
9 mo	0.636	0.546	0.211	0.556	0.166	0.235
12 mo	0.636	0.587	0.172	0.556	0.298	0.264
∞	0.636	0.590	0.166	0.556	0.456	0.213

	C. $\mathcal{R}_0 = 1.75$			D. $\mathcal{R}_0 = 1.25$		
	Deterministic	Stochastic		Deterministic	Stochastic	
t	I_t	$\mathbb{E}(I_t)$	$\sqrt{\mathbb{V}ar(I_t)}$	I_t	$\mathbb{E}(I_t)$	$\sqrt{\mathbb{V}ar(I_t)}$
1 wk	$2.9 * 10^{-7}$	$2.9 * 10^{-7}$	$2.8 * 10^{-7}$	$2.3 * 10^{-7}$	$2.3 * 10^{-7}$	$2.2 * 10^{-7}$
2 wk	$4.3 * 10^{-7}$	$4.3 * 10^{-7}$	$7.0 * 10^{-7}$	$2.6 * 10^{-7}$	$2.6 * 10^{-7}$	$4.3 * 10^{-7}$
4 wk	$9.0 * 10^{-7}$	$9.0 * 10^{-7}$	$3.2 * 10^{-6}$	$3.3 * 10^{-7}$	$3.3 * 10^{-7}$	$1.2 * 10^{-6}$
6 wk	$1.9 * 10^{-6}$	$1.9 * 10^{-6}$	$1.3 * 10^{-5}$	$4.3 * 10^{-7}$	$4.3 * 10^{-7}$	$3.0 * 10^{-6}$
8 wk	$4.0 * 10^{-6}$	$4.0 * 10^{-6}$	$5.3 * 10^{-5}$	$5.5 * 10^{-7}$	$5.5 * 10^{-7}$	$7.5 * 10^{-6}$
3 mo	$2.7 * 10^{-5}$	$2.6 * 10^{-5}$	$7.6 * 10^{-4}$	$1.0 * 10^{-6}$	$1.0 * 10^{-6}$	$5.2 * 10^{-5}$
4 mo	$1.4 * 10^{-4}$	$1.1 * 10^{-4}$	0.003	$1.8 * 10^{-6}$	$1.7 * 10^{-6}$	$1.6 * 10^{-4}$
6 mo	0.004	0.001	0.014	$5.2 * 10^{-6}$	$4.1 * 10^{-6}$	$5.4 * 10^{-4}$
9 mo	0.224	0.005	0.039	$2.7 * 10^{-5}$	$0.8 * 10^{-5}$	$1.1 * 10^{-3}$
12 mo	0.426	0.012	0.066	$1.4 * 10^{-4}$	$0.1 * 10^{-5}$	$1.4 * 10^{-3}$
18 mo	0.429	0.031	0.108	0.004	$8.9 * 10^{-6}$	$1.4 * 10^{-3}$
24 mo	0.429	0.050	0.135	0.063	$5.1 * 10^{-6}$	$1.1 * 10^{-3}$
36 mo	0.429	0.077	0.163	0.199	$1.3 * 10^{-6}$	$5.6 * 10^{-4}$
∞	0.429	0.131	0.197	0.20	0	0

number to 1.75 radically changes projections. Even at 24 months out, the conditional mean forecast is 5% with a (relatively) large conditional standard deviation of 13.5%. In contrast, in a deterministic model, the fraction infected with a reproduction number of 1.75 would be much higher: 42.6% of the entire population even in 12 months.

With $\mathcal{R}_0 = 1.25$, in our stochastic formulation, the disease goes into extinction on its own with probability one with no intervention nor vaccine. In contrast, the deterministic model predicts 20% of the US population to be infected in three years. Again, this significant conditional forecasts differences and opposite infection forecasts (extinction versus persistence) in the long run are due to the significant pandemic spread uncertainty (σ). In summary, heuristics garnered from a deterministic model can fundamentally skew cost and benefit assessments.

Infectious period of 10 days instead of 14 days. We also experimented with how our analysis changes if we assume that the average duration for an infected to be infective is 10 days, i.e., $\gamma = 1/10$ per day. The reproduction number is then 2.17. This is still a very high reproduction number. But our conclusions are similar to before. We omit these results for brevity.

Consequences of higher volatility σ. To see why transmission volatility matters so much when managing COVID-19 risks, it is useful to consider the impact of a higher volatility on the model's prediction. We choose $\sigma = 2$ per month.[21] In Figure 7, we plot the conditional distributions of I_t for $t = 1, 2, 4, 6, 8$ weeks and $9, 12, 18$ months. First, we see that for the near-term conditional distribution ($t = 1, 2$ weeks), the density is peaked close to zero. As we increase t, the density function shifts to the right and becomes flatter (for $t = 4, 6, 8$ weeks). As we further increase the forecasting horizon (e.g., to 9 and 12 months), we observe two modes for the conditional distribution. For example, for the one-year-ahead forecast: one mode is near zero (at $4.8 * 10^{-9}$) and the other mode is at 0.747.

[21] This value is in the 95% confidence interval for estimated σ^2, i.e. $(2.851 - 1.96 \times 2.537, 2.851 + 1.96 \times 2.537)$ based on the data of 16 regions from January to February (the mean of σ^2 is 2.851 and the standard deviation is 2.537).

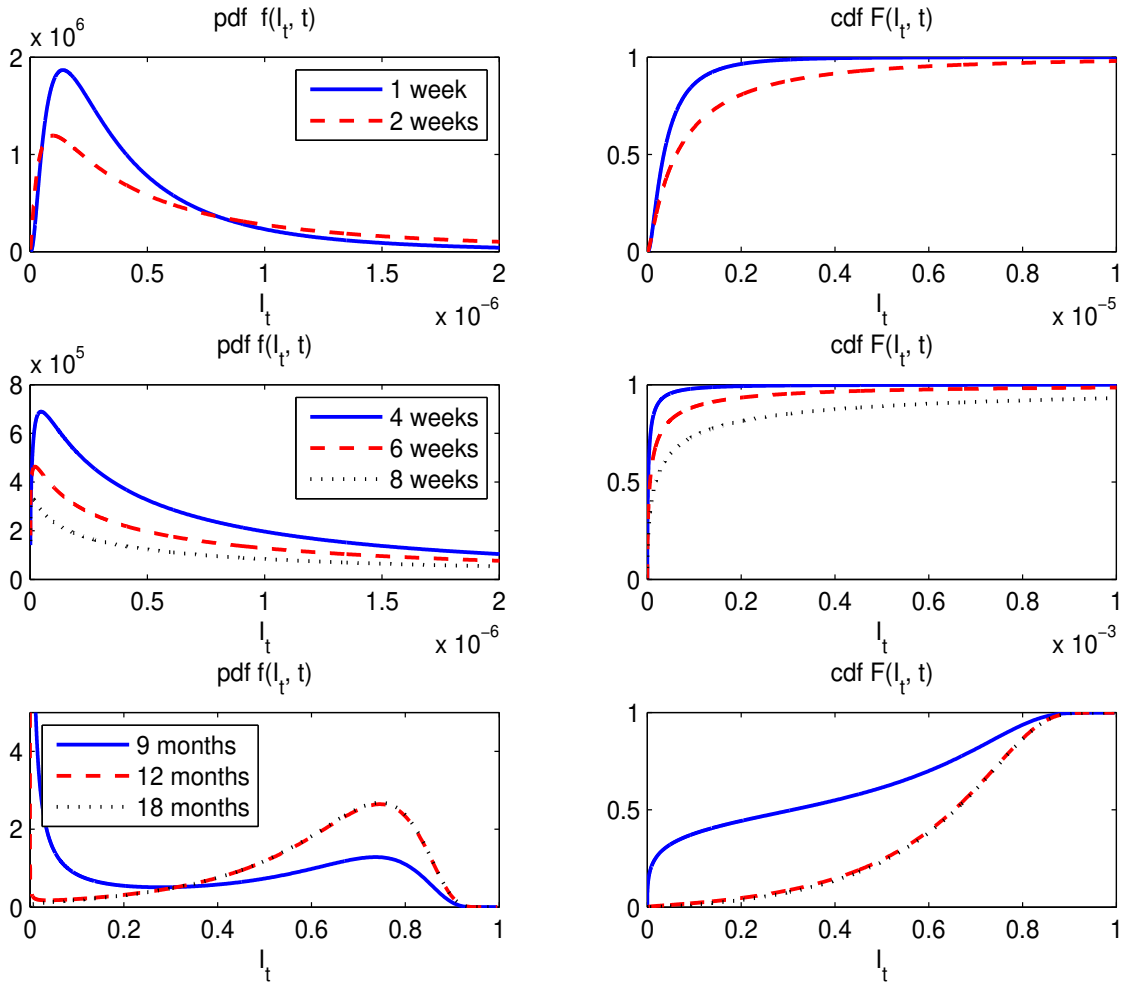

Figure 7: Conditional distributions of I_t with $I_0 = 2 \times 10^{-7}$ based on the US data as of March 1st.) Monthly parameter values are $\beta = 6.616$, $\gamma = 2.173$, $\sigma = 2$, and $\lambda = 0$.

It takes about one year and half for the conditional distribution to converge to the stochastic steady state where $I^{SS} = 0.630$ with a single mode at 0.747. Compared with the case where $\sigma = 1.689$, the drift $q(I)$ for the logarithmic infected $\ln(I)$ is substantially lower. As a result, the force (and hence the likelihood) for the mass I_t to move to the left is stronger when $\sigma = 2$ than when $\sigma = 1.689$. Also, we see that with a higher volatility, convergence to the stationary distribution also takes more time.

Table 4: Effects of Vaccine Arrival Rate, λ, on Conditional Distributions of I_t. Other parameter values are: $\beta = 6.616$, $\gamma = 2.173$, and $\sigma = 1.689$ per month with an implied value of $\mathcal{R}_0$, 3.045.

	A. Six Months			B. One Year		
	Deterministic	Stochastic		Deterministic	Stochastic	
t	I_t	$\mathbb{E}(I_t)$	$\sqrt{\mathbb{V}ar(I_t)}$	I_t	$\mathbb{E}(I_t)$	$\sqrt{\mathbb{V}ar(I_t)}$
1 wk	$5.4 * 10^{-7}$	$5.4 * 10^{-7}$	$5.4 * 10^{-7}$	$5.5 * 10^{-7}$	$5.5 * 10^{-7}$	$5.4 * 10^{-7}$
2 wk	$1.4 * 10^{-6}$	$1.4 * 10^{-6}$	$2.5 * 10^{-6}$	$1.5 * 10^{-6}$	$1.5 * 10^{-6}$	$2.5 * 10^{-6}$
4 wk	$1.0 * 10^{-5}$	$1.0 * 10^{-5}$	$4.0 * 10^{-5}$	$1.1 * 10^{-5}$	$1.1 * 10^{-5}$	$4.1 * 10^{-5}$
6 wk	$7.3 * 10^{-5}$	$7.3 * 10^{-5}$	$5.4 * 10^{-4}$	$8.2 * 10^{-5}$	$8.2 * 10^{-5}$	$5.7 * 10^{-4}$
8 wk	$5.2 * 10^{-4}$	$5.0 * 10^{-4}$	$4.5 * 10^{-3}$	$6.1 * 10^{-4}$	$5.8 * 10^{-4}$	$4.9 * 10^{-3}$
3 mo	0.061	0.019	0.076	0.078	0.024	0.085
4 mo	0.323	0.084	0.188	0.450	0.117	0.213
6 mo	0.248	0.191	0.294	0.408	0.314	0.321
9 mo	0.150	0.142	0.275	0.318	0.300	0.334
12 mo	0.091	0.086	0.225	0.247	0.235	0.321
24 mo	0.012	0.012	0.088	0.091	0.086	0.225
∞	0	0	0	0	0	0

	C. Two Years			D. Forty Months		
	Deterministic	Stochastic		Deterministic	Stochastic	
t	I_t	$\mathbb{E}(I_t)$	$\sqrt{\mathbb{V}ar(I_t)}$	I_t	$\mathbb{E}(I_t)$	$\sqrt{\mathbb{V}ar(I_t)}$
1 wk	$5.5 * 10^{-7}$	$5.5 * 10^{-7}$	$5.4 * 10^{-7}$	$5.6 * 10^{-7}$	$5.6 * 10^{-7}$	$5.4 * 10^{-7}$
2 wk	$1.5 * 10^{-6}$	$1.5 * 10^{-6}$	$2.5 * 10^{-6}$	$1.5 * 10^{-6}$	$1.5 * 10^{-6}$	$2.5 * 10^{-6}$
4 wk	$1.2 * 10^{-5}$	$1.2 * 10^{-5}$	$4.2 * 10^{-5}$	$1.2 * 10^{-5}$	$1.2 * 10^{-5}$	$4.2 * 10^{-5}$
6 wk	$8.7 * 10^{-5}$	$8.7 * 10^{-5}$	$5.9 * 10^{-4}$	$8.9 * 10^{-5}$	$8.9 * 10^{-5}$	$5.9 * 10^{-4}$
8 wk	$6.6 * 10^{-4}$	$6.3 * 10^{-4}$	$5.1 * 10^{-3}$	$6.8 * 10^{-4}$	$6.5 * 10^{-4}$	$5.1 * 10^{-3}$
3 mo	0.089	0.027	0.090	0.093	0.029	0.093
4 mo	0.531	0.138	0.225	0.568	0.148	0.230
6 mo	0.523	0.403	0.310	0.578	0.446	0.296
9 mo	0.462	0.437	0.321	0.537	0.507	0.289
12 mo	0.407	0.387	0.333	0.497	0.473	0.308
24 mo	0.247	0.235	0.320	0.369	0.350	0.336
36 mo	0.150	0.143	0.275	0.273	0.260	0.328
∞	0	0	0	0	0	0

Varying vaccine arrival rate λ. In Table 4, we calculate the impact of vaccine arrival on the conditional mean and standard deviation of I_t for varying expected arrival rates. For simplicity, we set $n(I) = 0$ for this calculation. While an eventual vaccine arrival will make the disease extinction, the conditional moments of I_t vary significantly with the expected arrival vaccine rate λ.

Panel A shows that if the vaccine is expected to arrive soon (e.g., six months), the current conditional forecast of I_t for any horizon t is much lower than without vaccine arrival and peaks around 6 months at 19%. Panel B shows that if the vaccine is expected to arrive in one year, the current conditional forecast of I_t for any horizon t is much lower than without vaccine arrival and also peaks around 6 months but obviously at a higher rate of 31.4%. Similarly, as we increase the expected waiting time for vaccine to two years (Panel C) or 40 months (Panel D), the expected infected fraction can reach as high as 44% and 51% around 9 months. These are very high numbers and indicate that waiting for vaccine to arrive will cause a very large fraction of the population to be infected, even though in the long run COVID-19 goes extinct in our model due to the eventual arrival of vaccine by assumption.

7 Stochastic Transmission Shocks and Financial Risks

While we have shown that $\mathcal{R}_0$ overstates the benefits of economy-wide lockdowns, we now show that it also mismeasures COVID-19 damage to financial markets. To do so, we analyze the quantitative effects of COVID-19 on earnings growth, the market price of pandemic risk, and vaccine arrival on valuation. Our strategy is to analyze each of these three effects in turn, so as to contrast how conclusions differ between the classic deterministic SIS model and our stochastic SIS model.

7.1 Earnings Growth Channel

In this subsection, we focus solely on the earnings growth channel by shutting down earnings volatility and market price of pandemic risk channels, $v(I_t) = 0$ and $\eta^z = 0$, and assuming that the vaccine arrival rate $\lambda = 0$. As a result, the pricing equation (20) is substantially

simplified as follows:

$$\left(r+\rho\phi\eta^{\mathcal{B}}-g(I)\right)p(I)=1+\left[\beta\left(1-I\right)-\gamma\right]Ip'(I)+\frac{(\sigma I(1-I))^2}{2}p''(I)\,, \tag{32}$$

where I impacts $p(I)$ via its drift and volatility effects on $g(I)$.

To contrast how valuation implications differ between deterministic and stochastic epidemic models, we choose key parameter values for our asset pricing model following the literature. We set the annual risk-free rate at 4%, the annual stock-market risk premium at 6%, and the annual stock market volatility at 20% (with an implied annual Sharpe ratio $\eta^{\mathcal{B}}=30\%$). Suppose that the asset's CAPM beta is one. Then, the cost of capital for this asset is equal to $4\%+1\times 6\%=10\%$. We set the (annual) earnings growth rate (in normal times), g_0, to 5%, so that we obtain a price-earnings ratio of $p_0=1/(10\%-5\%)=20$ in normal times.

We next specify the impact of the pandemic shock on the asset's earnings growth (drift) function $g(I_t)$ as follows:

$$g(I_t)=g_0\left(1-\zeta_1 I_t^{\zeta_2}\right)\,, \tag{33}$$

where $g_0>0$ is the drift in normal times. The two new parameters are ζ_1 and ζ_2. First, as $I_t=0$ is an absorbing state, we set $g(0)=g_0$ so that our pricing equation model is consistent with that under normal times. Second, earnings growth $g(I_t)$ is decreasing with I_t but at a slower rate as I_t increases implying $\zeta_1>0$ and $0<\zeta_2<1$. For our quantitative illustration, we focus on the parameter ζ_1, which captures the sensitivity of earnings growth to I.

Table 5 summarizes the parameter values used for our earnings growth channel analysis. We consider a range of values for ζ_1. We pay particular attention to severely affected industries such as airlines and hotels. The valuation of these industries collapsed by nearly 75% following the arrival of COVID-19. While there is no historical data with which we can nail down these parameters, we will intentionally pick a range of parameters to reflect the severity of the COVID-19 shock to these important industries. As our baseline we choose $\zeta_1=3$. As we demonstrate below, $\zeta_1=3$ corresponds to fairly mild long-run declines in growth rates of around 5%.

Table 5: This table summarizes the parameter values for our epidemic and asset valuation analyses assuming no pandemic price of risk and no vaccine arrival. Parameter values are based on one period being one month.

Parameters	Symbol	Value
A. Epidemic		
transmission rate	β	6.616
recovery rate	γ	2.173
volatility of infected population	σ	1.689
B. Asset pricing		
risk-free rate	r	4%/12
market price of business-as-usual risk	$\eta^{\mathcal{B}}$	30%/12
market price of pandemic risk	$\eta^{\mathcal{Z}}$	0
earnings growth volatility	ϕ	$20\%/\sqrt{12}$
correlation coefficient	ρ	1
normal-time earnings growth rate	g_0	5%/12
growth reduction level parameter	ζ_1	3
growth reduction curvature parameter	ζ_2	0.25
arrival rate of vaccine	λ	0

In Table 6, we report for the damage to valuations for this baseline case. This table is the economic damage analog to Table 3, which calculated the conditional expectations of infections, i.e. COVID-19 damage to health. We see in this table that COVID-19 damage for stock valuations also differs markedly between a deterministic versus a stochastic model.

The deterministic model would imply severe damage to valuation ratios for all the values of $\mathcal{R}_0$ greater than 1 (across Panels A-D). For instance, in Panel D for $\mathcal{R}_0 = 1.25$, the price-earnings ratio $p(I)$ is 7.64 in the beginning and dropping to 6.66 in the limit. That is, the valuation is substantially impaired according to deterministic model infection forecasts. The reason of course is that markets are forward looking and valuations are determined by cashflows discounted far into the future. The valuation damage becomes progressively worst as we move to higher levels of $\mathcal{R}_0$.

In sharp contrast, Panel D shows that when $\mathcal{R}_0$ is 1.25, our stochastic model predicts that

Table 6: Effects of Changing $\mathcal{R}_0$ on Conditional Distributions of $p(I_t)$ assuming no pandemic risk premium or vaccine. Other parameter values are: $\beta = 6.616$, $\gamma = 2.173$, and $\sigma = 1.689$ per month with an implied value of $\mathcal{R}_0$, 3.045.

	A. $\mathcal{R}_0 = 3.045$			B. $\mathcal{R}_0 = 2.25$		
	Deterministic	Stochastic		Deterministic	Stochastic	
t	$p(I_t)$	$\mathbb{E}(p(I_t))$	$\sqrt{\mathbb{V}ar(p(I_t))}$	$p(I_t)$	$\mathbb{E}(p(I_t))$	$\sqrt{\mathbb{V}ar(p(I_t))}$
1 wk	5.527	5.673	0.016	5.805	6.411	0.036
2 wk	5.513	5.660	0.022	5.791	6.399	0.051
4 wk	5.487	5.634	0.031	5.765	6.374	0.072
6 wk	5.461	5.608	0.037	5.739	6.349	0.088
8 wk	5.438	5.583	0.041	5.714	6.324	0.102
3 mo	5.393	5.527	0.044	5.654	6.263	0.131
4 mo	5.384	5.491	0.037	5.611	6.213	0.148
6 mo	5.384	5.461	0.015	5.572	6.121	0.160
9 mo	5.384	5.456	0.003	5.571	6.020	0.139
12 mo	5.384	5.456	0.002	5.571	5.964	0.104
∞	5.384	5.456	0.002	5.571	5.915	0.017

	C. $\mathcal{R}_0 = 1.75$			D. $\mathcal{R}_0 = 1.25$		
	Deterministic	Stochastic		Deterministic	Stochastic	
t	$p(I_t)$	$\mathbb{E}(p(I_t))$	$\sqrt{\mathbb{V}ar(p(I_t))}$	$p(I_t)$	$\mathbb{E}(p(I_t))$	$\sqrt{\mathbb{V}ar(p(I_t))}$
1 wk	6.215	12.670	0.337	7.640	19.966	0.008
2 wk	6.202	12.664	0.477	7.628	19.967	0.011
4 wk	6.176	12.651	0.678	7.606	19.969	0.014
6 wk	6.151	12.639	0.834	7.583	19.971	0.017
8 wk	6.126	12.627	0.967	7.560	19.973	0.019
3 mo	6.064	12.595	1.245	7.504	19.977	0.022
4 mo	6.013	12.567	1.439	7.455	19.980	0.023
6 mo	5.920	12.502	1.737	7.357	19.985	0.024
9 mo	5.843	12.382	2.024	7.215	19.990	0.022
12 mo	5.836	12.247	2.195	7.077	19.993	0.020
18 mo	5.836	11.969	2.359	6.838	19.996	0.014
24 mo	5.836	11.713	2.402	6.691	19.997	0.010
36 mo	5.836	11.298	2.343	6.656	19.997	0.006
∞	5.836	10.446	1.813	6.656	20	0

the expected price-earnings ratios at all horizons are above 19.9, barely different from the $p_0 = 20$ benchmark for the case with no COVID-19. The reason is that infection forecasts in our stochastic model are only slightly above zero, (the largest value of I_t is $0.8 * 10^{-5}$ as we demonstrated in Panel D of Table 3.) These low values of I_t means that the epidemic breaks out with zero probability and is due to σ being significant. This markedly different forecasts of I_t dynamics between the deterministic model and our stochastic epidemic model explains the valuation differences implied by these two models. s

As we increase $\mathcal{R}_0$ to 1.75 (Panel C), we can see that there is now damage to valuation even for our stochastic model. Since markets are forward-looking, we see significant economic damage to valuation ratios in week 1 after COVID-19's arrival—the price-earnings ratio declines to 12.67, which is a significant drop from the pre-COVID-19 value of 20. Moreover, valuations ratios continue to drop over time, reaching a steady-state of 10.45 as infected masses increase.

As $\mathcal{R}_0$ continues to rise in Panels A and B, we see that valuation ratios get closer to the predictions from the deterministic model. Nonetheless, even at our estimate of a reproduction number of 3.045 for COVID-19 (i.e. the scenario in Panel A), predictions are not exactly the same across the two models.

In Figure 8, we plot $p(I)$ and $g(I)$ for various values of ζ_1. The $p(I)$ plots are graphical illustrations of how results from Table 3 change as we move away from our baseline case with $\zeta_1 = 3$, assuming an $\mathcal{R}_0 = 3.045$. We see increasingly severe damage to valuations as ζ_1 increases. The effects are highly non-linear in ζ_1. We can see how $g(I)$ declines with I but non-linearly. This non-linearity essentially imparts a non-linearity of economic damage to valuation with $\mathcal{R}_0$. The drop in the valuation ratio occurs for even low levels of infection given that markets are forward-looking. To see this result more clearly, we plot $p(I)$ and $g(I)$ with respect to $\ln(I)$ on the horizontal axis in Panels C and D. The damage to valuation is convex in I.

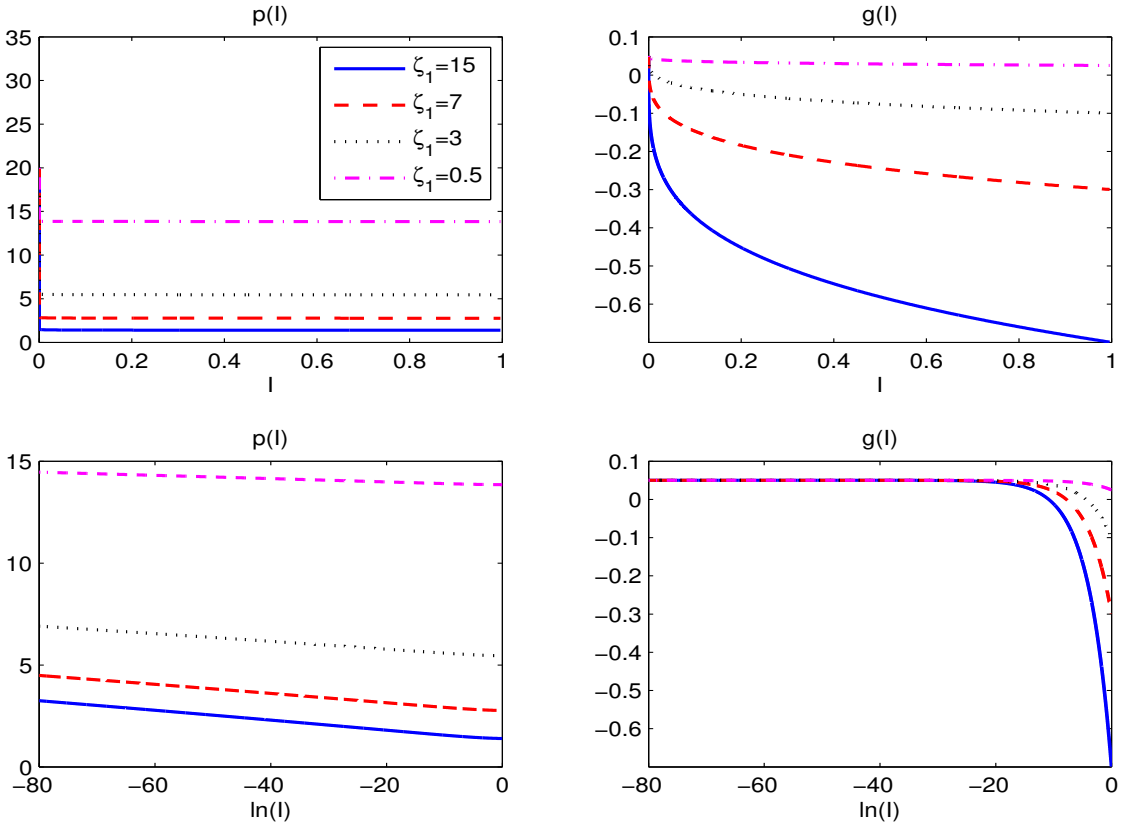

Figure 8: Effects of Changing ζ_1 on price-earnings ratio $p(I)$ and the expected earnings growth rate $g(I)$. Panels A and B plot against $I \in [0,1]$ and Panels C and D plot against $\ln I \in (-\infty, 0]$. Other parameter values are: $\beta = 6.616$, $\gamma = 2.173$, and $\sigma = 1.689$ per month with an implied value of $\mathcal{R}_0$, 3.045.

7.2 Market Price of Pandemic Risk

Next, we evaluate the impact of market price of pandemic risk on the conditional mean and standard deviation of I_t for varying values of $\eta^{\mathcal{Z}}$. For simplicity, we set $v(I) = 0$ so that the pricing equation (20) is simplified as follows:

$$\left(r + \rho\phi\eta^{\mathcal{B}} - g(I)\right) p(I) = 1 + \left[\beta^{\mathbb{Q}}(1-I) - \gamma\right] I p'(I) + \frac{(\sigma I(1-I))^2}{2} p''(I)\,, \tag{34}$$

where we use $\beta^{\mathbb{Q}} = \beta - \sigma\eta^{\mathcal{Z}}$ rather than β for the valuation purpose (the key difference from the analysis in the preceding subsection.) That is, we under-estimate the impact of pandemic risk on valuation, as we ignore two correction terms involving $v(I)$ in (20).

In Table 7, we choose $\mathcal{R}_0 = 1.25$ to make the point that even if the disease is mildly con-

Table 7: Effects of Changing $\eta^{\mathcal{Z}}$ on Conditional Distributions of $p(I_t)$. Here, $\mathcal{R}_0 = 1.25$ (as $\beta = 2.716$, $\gamma = 2.173$ and $\sigma = 1.689$ per month) and $\lambda = 0$. The risk-adjusted transmission rate is $\beta^{\mathbb{Q}} = \beta - \eta^{\mathcal{Z}}\sigma$.

	A. $\beta^{\mathbb{Q}}/\beta = 1$ $(\eta^{\mathcal{Z}} = 0)$			B. $\beta^{\mathbb{Q}}/\beta = 1.5$ $(\eta^{\mathcal{Z}} = -2.786)$		
	Deterministic	Stochastic		Deterministic	Stochastic	
t	$p(I_t)$	$\mathbb{E}(p(I_t))$	$\sqrt{\mathbb{V}ar(p(I_t))}$	$p(I_t)$	$\mathbb{E}(p(I_t))$	$\sqrt{\mathbb{V}ar(p(I_t))}$
1 wk	7.640	19.966	0.008	7.640	8.761	0.206
2 wk	7.628	19.967	0.011	7.628	8.832	0.314
4 wk	7.606	19.969	0.014	7.606	8.993	0.525
6 wk	7.583	19.971	0.017	7.583	9.183	0.770
8 wk	7.560	19.973	0.019	7.560	9.409	1.070
3 mo	7.504	19.977	0.022	7.504	10.131	1.954
4 mo	7.455	19.980	0.023	7.455	10.875	2.625
6 mo	7.357	19.985	0.024	7.357	12.310	3.370
9 mo	7.215	19.990	0.022	7.215	13.840	3.543
12 mo	7.077	19.993	0.020	7.077	14.719	3.360
24 mo	6.691	19.997	0.010	6.691	15.696	2.834
36 mo	6.656	19.997	0.006	6.656	15.797	2.751
∞	6.656	20	0	6.656	20	0

	C. $\beta^{\mathbb{Q}}/\beta = 2$ $(\eta^{\mathcal{Z}} = -5.571)$			D. $\beta^{\mathbb{Q}}/\beta = 3$ $(\eta^{\mathcal{Z}} = -11.142)$		
	Deterministic	Stochastic		Deterministic	Stochastic	
t	$p(I_t)$	$\mathbb{E}(p(I_t))$	$\sqrt{\mathbb{V}ar(p(I_t))}$	$p(I_t)$	$\mathbb{E}(p(I_t))$	$\sqrt{\mathbb{V}ar(p(I_t))}$
1 wk	7.640	6.058	0.025	7.640	5.486	0.011
2 wk	7.628	6.065	0.036	7.628	5.488	0.015
4 wk	7.606	6.078	0.055	7.606	5.494	0.021
6 wk	7.583	6.097	0.118	7.583	5.499	0.050
8 wk	7.560	6.130	0.310	7.560	5.509	0.165
3 mo	7.504	6.365	1.155	7.504	5.595	0.719
4 mo	7.455	6.754	1.924	7.455	5.765	1.255
6 mo	7.357	7.700	2.969	7.357	6.211	2.052
9 mo	7.215	8.830	3.593	7.215	6.763	2.644
12 mo	7.077	9.500	3.767	7.077	7.094	2.894
24 mo	6.691	10.245	3.815	6.691	7.462	3.107
∞	6.656	20	0	6.656	20	0

tagious, its impact on valuation could still be substantial when the market price of pandemic risk causes the risk-adjusted transmission rate $\beta^{\mathbb{Q}}$ to be significantly larger from β.

Panel A shows that if investors attach zero market price of pandemic risk, i.e., $\eta^{\mathcal{Z}} = 0$, I_t essentially has no impact on $p(I)$. But introducing market price of pandemic risk, e.g., setting $\eta^{\mathcal{Z}}$ to -5.571, so that $\beta^{\mathbb{Q}} = 2 \times \beta = 5.43$, significantly damages valuation. For example, valuation forecasts for the first three months on average drop by about 70% and two-year-ahead forecast decreases to about half of the price-earnings ratio in normal times, $p_0 = 20$. Note that even if the basic reproduction number is only 1.25 and the pandemic goes into extinction with no intervention in the long run on its own, for valuation purposes, risk-averse investors may still attach a high risk premium so that they view the epidemic is persistent after risk adjustment (i..e, under the risk-neutral measure $\mathbb{Q}$). As a result, valuation is much reduced. That is, health and financial health implications can be quite different.

Additionally and perhaps surprisingly, the forecast of $p(I_t)$ as a function of time horizon t in the stochastic model is opposite to that in the deterministic model. In the deterministic model, $p(I_t)$ decreases with t as I_t increases over time. In contrast, in our stochastic model, the conditional forecast $\mathbb{E}(p(I_t))$ increases with t as the disease eventually goes extinct, even though $\mathcal{R}_0 = 1.25$ and hence the growth rate $g(I_t)$ rebounds in our stochastic model (despite the market price of pandemic risk).

7.3 Valuing Potential Arrival of Vaccine

Finally, we show that the expectation of vaccine arrival in the foreseeable future (compared with the no-vaccine scenario) significantly mitigates the negative impact of COVID-19 on valuation. For our illustration, we choose $\lambda^{\mathbb{Q}}/\lambda = 1/2$ and equivalently $\kappa = -\ln 2$. That is, risk-averse investors perceive the arrival rate for pricing purposes, $\lambda^{\mathbb{Q}}$ at the half of λ, the (physical) vaccine arrival rate. For simplicity, we set $n(I) = 0$ in this subsection.

In Table 8, we calculate the value of a vaccine arrival by using $p(I_t)$ for the four scenarios, where the expected arrival time for vaccine is six months, one year, two years, and forty

Table 8: Effects of Changing Vaccine Arrival Rate, λ, on Conditional Distributions of $p(I_t)$. Other parameter values are: $\beta = 6.616$, $\gamma = 2.173$, and $\sigma = 1.689$ per month with an implied value of $\mathcal{R}_0$, 3.045. Panels A, B, C, and D correspond to the expected vaccine arrival time to be six months, one year, two years, and forty months.

	A. Six Months			B. One Year		
	Deterministic	Stochastic		Deterministic	Stochastic	
t	$p(I_t)$	$\mathbb{E}(p(I_t))$	$\sqrt{\mathbb{V}ar(p(I_t))}$	$p(I_t)$	$\mathbb{E}(p(I_t))$	$\sqrt{\mathbb{V}ar(p(I_t))}$
1 wk	18.201	18.405	0.318	16.511	16.750	0.454
2 wk	18.235	18.435	0.445	16.542	16.779	0.639
4 wk	18.303	18.494	0.617	16.605	16.837	0.896
6 wk	18.370	18.553	0.741	16.670	16.896	1.088
8 wk	18.438	18.611	0.838	16.737	16.956	1.244
3 mo	18.627	18.759	1.002	16.935	17.116	1.538
4 mo	18.821	18.895	1.075	17.159	17.273	1.712
6 mo	19.155	19.175	1.080	17.596	17.640	1.898
9 mo	19.487	19.495	0.939	18.126	18.154	1.948
12 mo	19.690	19.695	0.771	18.544	18.565	1.881
24 mo	19.958	19.959	0.302	19.464	19.472	1.334
∞	20	20	0	20	20	0

	C. Two Years			D. Forty Months		
	Deterministic	Stochastic		Deterministic	Stochastic	
t	$p(I_t)$	$\mathbb{E}(p(I_t))$	$\sqrt{\mathbb{V}ar(p(I_t))}$	$p(I_t)$	$\mathbb{E}(p(I_t))$	$\sqrt{\mathbb{V}ar(p(I_t))}$
1 wk	14.181	14.430	0.548	12.269	12.512	0.570
2 wk	14.204	14.453	0.774	12.285	12.527	0.805
4 wk	14.252	14.498	1.090	12.318	12.558	1.137
6 wk	14.302	14.544	1.330	12.352	12.591	1.391
8 wk	14.355	14.592	1.530	12.390	12.624	1.603
3 mo	14.520	14.725	1.925	12.515	12.722	2.030
4 mo	14.722	14.863	2.183	12.680	12.830	2.320
6 mo	15.145	15.216	2.546	13.038	13.123	2.763
9 mo	15.714	15.768	2.850	13.540	13.610	3.205
12 mo	16.221	16.269	3.005	14.010	14.075	3.505
24 mo	17.708	17.737	2.967	15.563	15.611	3.980
∞	20	20	0	20	20	0

months, respectively.[22] We can see that the price-earnings ratio $p(I_t)$ does not fall nearly as much when there is a potential for a vaccine in half year or one year (Panels A and B). However, valuations begin to get significantly impacted even if the expected vaccine arrival time is two years or forty months out as we see in Panels C and D, respectively. This is due to a combination of both a longer expected waiting time and a risk premium for stochastic vaccine arrival.

Importantly, we can relate these benefits to those obtained through government intervention regarding β and reproduction number. For example, consider the conditional forecast of $p(t)$ for horizons up to one year. The economic benefits of targeting a reproduction number around 1.75 (shown in Panel C of Table 6) is roughly in line with having a vaccine expected to arrive in forty months (Panel D).

8 Conclusion

We propose a parsimonious epidemic model that highlights the importance of transmission-rate shocks due to unpredictable environmental factors. The model is a three-parameter nonlinear diffusion process amenable for risk-management applications in areas such as economics and finance. We integrate the model into an asset-pricing framework that accounts for a potential vaccine so that we can quantify the financial damage of COVID-19 and relate this damage to epidemic data. Our model has a number of implications for the usefulness of the basic reproduction number.

In short, our contribution is to demonstrate how analysis of pandemics fundamentally differs when using a stochastic epidemic model as opposed to relying on the classic deterministic epidemic model and the $\mathcal{R}_0$ heuristic as an approximation. Our stochastic epidemic model is tractable enough that it can be used for further analysis such as stochastic control of pandemics. At the same time, it generates testable predictions that might be of interest to empiricists. We leave these avenues for future research.

[22] Note that we ignore the market price of pandemic risk by setting $\eta^{\mathcal{Z}} = 0$.

Appendices

A Estimation

Estimation of β. We use ordinary least squares (OLS) method to estimate the parameter β for a given value of γ. Discretizing I_t in (6) gives

$$I_{t+\Delta} = I_t + (\beta(1-I_t)-\gamma)I_t\Delta + \sigma\, I_t(1-I_t)\sqrt{\Delta}\,\epsilon_{t+\Delta}\,, \tag{A.35}$$

where Δ is the time increment, $\epsilon_{t+\Delta}$ is a standard normal random variable, and

$$\frac{(\frac{I_{t+\Delta}}{I_t}-1)-(\beta(1-I_t)-\gamma)\Delta}{1-I_t} = \sigma\sqrt{\Delta}\,\epsilon_{t+\Delta} \sim \mathcal{N}(0,\sigma^2\Delta)\,. \tag{A.36}$$

Let N denote the sample size. We choose an estimate of β to minimize the following:

$$\Sigma_{i=0}^{N-2}\left(\frac{(\frac{I_{(i+1)\Delta}}{I_{i\Delta}}-1)-(\beta(1-I_{i\Delta})-\gamma)\Delta}{1-I_{i\Delta}}\right)^2\,. \tag{A.37}$$

Setting Δ to one in (A.37) yields $\widehat{\beta}$, which is given by (28). The variance of $\widehat{\beta}$ is given by

$$\mathbb{V}ar(\widehat{\beta}) \;=\; \mathbb{E}(\widehat{\beta}-\beta)^2 = \mathbb{E}\left(\frac{1}{N-1}\Sigma_0^{N-2}\frac{\frac{I_{i+1}}{I_i}-1+\gamma}{1-I_i}-\beta\right)^2 = \frac{\sigma^2}{N-1}\,. \tag{A.38}$$

The 95% confidence interval for $\widehat{\beta}$ is $\left(\widehat{\beta}-1.96\frac{\sigma}{\sqrt{N-1}},\widehat{\beta}+1.96\frac{\sigma}{\sqrt{N-1}}\right)$.

Estimation of σ^2. Equation (9) implies that the quadratic variation of $\ln I_t$, which we denote by $<\ln I_t, \ln I_t>$, satisfies $d<\ln I_t, \ln I_t> = (1-I_t)^2\sigma^2 dt$. Therefore, we have

$$\sigma^2 = \frac{<\ln I_t, \ln I_t>}{\int_0^t (1-I_s)^2 ds}\,. \tag{A.39}$$

Discretizing the preceding equation, we obtain the following estimate of σ^2:

$$\widehat{\sigma}^2 = \frac{\Sigma_{i=0}^{N-2}(\ln I_{(i+1)\Delta} - \ln I_{i\Delta})^2}{\Sigma_{i=0}^{N-2}(1-I_{i\Delta})^2\Delta}\,. \tag{A.40}$$

By setting Δ to one, we obtain (29).

B Deterministic SIS Model

Consider the case where $\beta \neq \gamma$. (The case with $\beta = \gamma$ is straightforward.) We have

$$\frac{dI_t}{dt} = \left[\frac{\beta}{\beta-\gamma}\left(e^{(\beta-\gamma)t/2} - e^{-(\beta-\gamma)t/2}\right) + \frac{1}{I_0}e^{-(\beta-\gamma)t/2}\right]^{-2}\left(\frac{1}{I_0} - \frac{\beta}{\beta-\gamma}\right)(\beta-\gamma) \quad \text{(B.41)}$$

The second derivative of I_t is

$$\begin{aligned}\frac{d^2I_t}{dt^2} &= -2\left[\frac{\beta}{\beta-\gamma}\left(e^{(\beta-\gamma)t/2} - e^{-(\beta-\gamma)t/2}\right) + \frac{1}{I_0}e^{-(\beta-\gamma)t/2}\right]^{-3}\left(\frac{1}{I_0} - \frac{\beta}{\beta-\gamma}\right)(\beta-\gamma) \\ &\quad \times\left[\frac{\beta}{2}e^{(\beta-\gamma)t/2} + \left(\frac{\beta}{2} - \frac{\beta-\gamma}{2}\frac{1}{I_0}\right)e^{-(\beta-\gamma)t/2}\right]. \quad \text{(B.42)}\end{aligned}$$

Let t^* denote the time at which the peak of the net change dI_t/dt is reached, i.e., when $d^2I_t/dt^2 = 0$. It is immediate to conclude that the curve dI_t/dt peaks at t^* where

$$t^* = \frac{1}{(\beta-\gamma)}\ln\left(\frac{\beta-\gamma}{\beta}\frac{1}{I_0} - 1\right) = \frac{1}{(\beta-\gamma)}\ln\left(\left(1 - \frac{1}{\mathcal{R}_0}\right)\frac{1}{I_0} - 1\right) \quad \text{(B.43)}$$

C Derivation Details for Pricing and Hedging

Let P denote the value of the asset. The standard asset-pricing theorem implies that the following holds (Duffie, 2001):

$$P_t = \mathbb{E}_t\left(\int_t^\infty \frac{\mathbb{M}_s}{\mathbb{M}_t}Y_s\,ds\right) = \mathbb{E}_t^{\mathbb{Q}}\left(\int_t^\infty e^{-r(s-t)}Y_s\,ds\right), \quad \text{(C.44)}$$

where the first pricing equation is under the physical (real-world) probability measure $\mathbb{P}$ and the second pricing equation is under the risk-neutral (which means risk-adjusted) probability measure $\mathbb{Q}$. It is convenient to use $\mathbb{Q}$ for pricing purposes.

Risk-neutral dynamics. Let $\mathcal{B}_t^{\mathbb{Q}}$ and $\mathcal{Z}_t^{\mathbb{Q}}$ denote the standard Brownian motions for the business-as-usual and pandemic shocks, respectively. By using Girsanov's Theorem, we have the following relations between them under $\mathbb{Q}$ and the real-world (physical) measure $\mathbb{P}$:

$$\begin{aligned}d\mathcal{B}_t^{\mathbb{Q}} &= d\mathcal{B}_t + \eta^{\mathcal{B}}dt \quad \text{(C.45)}\\ d\mathcal{Z}_t^{\mathbb{Q}} &= d\mathcal{Z}_t + \eta^{\mathcal{Z}}dt\,. \quad \text{(C.46)}\end{aligned}$$

We thus may write the dynamics for I under the risk-neutral measure $\mathbb{Q}$ as follows:

$$\begin{aligned}dI_t &= \left[\beta(1-I_t) - \gamma - \eta^{\mathcal{Z}}\sigma\,(1-I_t)\right]I_t\,dt + \sigma\,I_t(1-I_t)\,d\mathcal{Z}_t^{\mathbb{Q}} \quad \text{(C.47)}\\ &= \left[\beta^{\mathbb{Q}}\,(1-I_t) - \gamma\right]I_t\,dt + \sigma\,I_t(1-I_t)\,d\mathcal{Z}_t^{\mathbb{Q}}\,, \quad \text{(C.48)}\end{aligned}$$

where $\beta^{\mathbb{Q}} = \beta - \eta^{\mathcal{Z}}\sigma$.

The earnings process under the risk-neutral measure $\mathbb{Q}$ is:

$$\frac{dY_t}{Y_t} = g^{\mathbb{Q}}(I_t)dt + v(I_t)\, d\mathcal{Z}_t^{\mathbb{Q}} + \rho\phi\, d\mathcal{B}_t^{\mathbb{Q}} + \sqrt{1-\rho^2}\,\phi\, d\mathcal{W}_t\,, \tag{C.49}$$

where the (risk-adjusted) earnings growth rate $g^{\mathbb{Q}}(I_t)$ is given by:

$$g^{\mathbb{Q}}(I_t) = g(I_t) - v(I_t)\eta^{\mathcal{Z}} - \rho\phi\eta^{\mathcal{B}}\,. \tag{C.50}$$

Note that both business-as-usual and pandemic risks appear in (C.50).

Pricing. The fundamental theorem of asset pricing (Duffie, 2001) implies that

$$\begin{aligned} rP(Y,I) &= Y + \left[g(I) - v(I)\eta^{\mathcal{Z}} - \rho\phi\eta^{\mathcal{B}}\right] Y P_Y(Y,I) + \frac{1}{2}\left[v(I)^2 + \phi^2\right] Y^2 P_{YY}(Y,I) \\ &\quad + \left[\left(\beta - \eta^{\mathcal{Z}}\sigma\right)(1-I) - \gamma\right] I P_I(Y,I) + \frac{1}{2}\sigma^2 I^2 (1-I)^2 P_{II}(Y,I) \\ &\quad + P_{IY}\sigma\, I(1-I)v(I)Y\,. \end{aligned} \tag{C.51}$$

As $P(Y_t, I_t) = p(I_t)Y_t$, we have $P_Y(Y,I) = p(I)$, $P_{YY}(Y,I) = 0$, $P_I(Y,I) = p'(I)Y$, $P_{II}(Y,I) = p''(I)Y$, and $P_{IY}(Y,I) = p'(I)$. Substituting these expressions into (C.51) yields

$$\begin{aligned} rp(I) &= 1 + \left[g(I) - v(I)\eta^{\mathcal{Z}} - \rho\phi\eta^{\mathcal{B}}\right] p(I) + \left[\left(\beta - \eta^{\mathcal{Z}}\sigma\right)(1-I) - \gamma\right] I p'(I) \\ &\quad + \frac{1}{2}\sigma^2 I^2 (1-I)^2 p''(I) + p'(I)\sigma\, I(1-I)v(I)\,. \end{aligned} \tag{C.52}$$

Re-organizing (C.52) yields (20).

Return dynamics. The asset's cum-dividend return process is given by

$$\begin{aligned} \frac{Y_t dt + dP_t}{P_t} &= \frac{dt}{p(I_t)} + \frac{dY_t}{Y_t} + \frac{dp(I_t)}{p(I_t)} + \frac{d < p(I_t), Y_t >}{p(I_t)Y_t} \\ &= \frac{1}{p(I_t)} + \frac{dY_t}{Y_t} + \frac{1}{p(I_t)}\left(p'(I_t)dI_t + \frac{p''(I_t) < dI_t, dI_t >}{2}\right) + \frac{p'(I_t) < dI_t, dY_t >}{p(I_t)Y_t} \\ &= (r + \theta(I_t))dt + \sigma_R^{\mathcal{Z}}(I_t)\, d\mathcal{Z}_t + \rho\phi\, d\mathcal{B}_t + \sqrt{1-\rho^2}\,\phi\, d\mathcal{W}_t\,, \end{aligned} \tag{C.53}$$

where $\sigma_R^{\mathcal{Z}}(I_t)$ is the asset's return volatility (due to pandemic risk) given by

$$\sigma_R^{\mathcal{Z}}(I_t) = v(I_t) + \frac{p'(I_t)}{p(I_t)} I_t(1-I_t)\sigma \tag{C.54}$$

and $\theta(I_t)$ is the asset's expected excess return (over the risk-free rate r) given by

$$\theta(I_t) = \rho\phi\,\eta^{\mathcal{B}} + \sigma_R^{\mathcal{Z}}(I_t)\eta^{\mathcal{Z}}\,. \tag{C.55}$$

Pandemic Risk and Risk Premium. There are two terms in return volatility loading due to pandemic risk, $\sigma_R^{\mathcal{Z}}(I_t)$. The first term is the direct effect of pandemic shocks on the asset's cash-flow risk. The second term in (C.54) captures the sensitivity of the equilibrium pricing-earnings ratio $p(I_t)$ with respect to I_t due to the correlation between the SDF and pandemic shocks.

The asset's expected excess return $\theta(I_t)$ given in (C.55) has two components. The first in $\theta(I_t)$ is the standard term (e.g., implied by CAPM as we discussed earlier) in the absence of pandemic shocks. The key for our analysis is the second term, which is equal to the product of the market price of pandemic risk $\eta^{\mathcal{Z}}$ and the quantity (volatility) of pandemic risk $\sigma_R^{\mathcal{Z}}$ defined in (C.54).

Next, we incorporate the risk premium for vaccine arrival. The fundamental theorem of asset pricing implies that the asset's value, $P(Y, I)$, satisfies the following pricing equation:

$$\begin{aligned} rP(Y,I) &= Y + \left[g(I) - v(I)\eta^{\mathcal{Z}} - \rho\phi\eta^{\mathcal{B}}\right] Y P_Y(Y,I) + \frac{1}{2}\left[v(I)^2 + \phi^2\right] Y^2 P_{YY}(Y,I) \\ &\quad + \left[\left(\beta - \eta^{\mathcal{Z}}\sigma\right)(1-I) - \gamma\right] I P_I(Y,I) + \frac{1}{2}\sigma^2 I^2 (1-I)^2 P_{II}(Y,I) \\ &\quad + P_{IY}\sigma\, I(1-I)v(I)Y + \lambda^{\mathbb{Q}}(P(Y,0) - P(Y,I))\,. \end{aligned} \tag{C.56}$$

Substituting $P(Y_t, I_t) = p(I_t)Y_t$ into (C.56), we obtain the pricing equation (26) for $p(I_t)$.

References

Adda, J., 2016. Economic activity and the spread of viral diseases: Evidence from high frequency data. *The Quarterly Journal of Economics*, 131(2), pp.891-941.

Almond, D., 2006. Is the 1918 influenza pandemic over? Long-term effects of in utero influenza exposure in the post-1940 US population. *Journal of Political Economy*, 114(4), pp.672-712.

Andersson, H., and Britton, T. 2012. *Stochastic epidemic models and their statistical analysis* (Vol. 151). Springer Science and Business Media.

Alvarez, F.E., Argente, D. and Lippi, F., 2020. A simple planning problem for covid-19 lockdown (No. w26981). National Bureau of Economic Research.

Atkeson, A., 2020. What will be the economic impact of COVID-19 in the US? Rough estimates of disease scenarios (No. w26867). National Bureau of Economic Research.

Black, F. and Scholes, M., 1973. The pricing of options and corporate liabilities. *Journal of Political Economy*, 81(3), pp.637-654.

Brauer, F., Driessche, P.D. and Wu, J., 2008. *Lecture Notes in Mathematical Epidemiology*. Berlin, Germany: Springer.

Cochrane, J.H., 2009. *Asset Pricing: Revised Edition*. Princeton university press.

Duffie, D., 2001. *Dynamic Asset Pricing Theory*. Princeton University Press.

Dureau, J., Kalogeropoulos, K. and Baguelin, M., 2013. Capturing the time-varying drivers of an epidemic using stochastic dynamical systems. *Biostatistics*, 14(3), pp.541-555.

Eichenbaum, M.S., Rebelo, S. and Trabandt, M., 2020. The macroeconomics of epidemics (No. w26882). National Bureau of Economic Research.

Federal Reserve Board, *Financial Stability Report*, May 15, 2020.

Fernández-Villaverde, J. and Jones, C.I., 2020. Estimating and Simulating a SIRD Model of COVID-19 for Many Countries, States, and Cities.

Ferguson, N., Laydon, D., Nedjati Gilani, G., Imai, N., Ainslie, K., Baguelin, M., Bhatia, S., Boonyasiri, A., Cucunuba Perez, Z.U.L.M.A., Cuomo-Dannenburg, G. and Dighe, A., 2020. Report 9: Impact of non-pharmaceutical interventions (NPIs) to reduce COVID-19 mortality and healthcare demand.

Gormsen, N.J. and Koijen, R.S., 2020. Coronavirus: Impact on stock prices and growth expectations. University of Chicago, Becker Friedman Institute for Economics Working Paper, (2020-22).

Gourinchas, P.O., 2020. Flattening the pandemic and recession curves. Mitigating the COVID Economic Crisis: Act Fast and Do Whatever, Working Paper, p.31.

Gray, A., Greenhalgh, D., Hu, L., Mao, X. and Pan, J., 2011. A stochastic differential equation SIS epidemic model. *SIAM Journal on Applied Mathematics*, 71(3), pp.876-902.

Hsiang, S., Allen, D., Annan-Phan, S., Bell, K., Bolliger, I., Chong, T., Druckenmiller, H., Hultgren, A., Huang, L.Y., Krasovich, E. and Lau, P., 2020. The Effect of Large-Scale Anti-Contagion Policies on the Coronavirus (COVID-19) Pandemic. medRxiv.

Imai, N., Cori, A., Dorigatti, I., Baguelin, M., Donnelly, C.A., Riley, S. and Ferguson, N.M., 2020. Report 3: transmissibility of 2019-nCoV. Reference Source.

Kermack, W.O. and McKendrick, A.G., 1927. A contribution to the mathematical theory of epidemics. *Proceedings of the Royal Society of London. Series A, Containing Papers of a Mathematical and Physical Character*,115(772), pp.700-721.

Kucharski, A.J., Russell, T.W., Diamond, C., Liu, Y., Edmunds, J., Funk, S., Eggo, R.M., Sun, F., Jit, M., Munday, J.D. and Davies, N., 2020. Early dynamics of transmission and control of COVID-19: a mathematical modelling study. *The Lancet Infectious Diseases*.

Lucas Jr, R.E., 1978. Asset prices in an exchange economy. *Econometrica: Journal of the Econometric Society*, pp.1429-1445.

Li, R., Pei, S., Chen, B., Song, Y., Zhang, T., Yang, W. and Shaman, J., 2020. Substantial undocumented infection facilitates the rapid dissemination of novel coronavirus (SARS-CoV-2). *Science*, 368(6490), pp.489-493.

Merton, R.C., 1973. An intertemporal capital asset pricing model. *Econometrica: Journal of the Econometric Society*, pp.867-887.

Newman, M., 2018. Networks. Oxford University Press.

Sharpe, W.F., 1964. Capital asset prices: A theory of market equilibrium under conditions of risk. *The Journal of Finance*, 19(3), pp.425-442.

Toda, A.A., 2020. Susceptible-infected-recovered (SIR) dynamics of COVID-19 and economic impact. arXiv preprint arXiv:2003.11221.